Seismic Behaviour Assessment of Eccentrically Split-X Braced Frames

Ramin Sheykhi[1], Nader Fanaie[*2]

[1]Graduated Student, Department of Civil Engineering, K. N. Toosi University of Technology, Tehran, Iran

[2]Associate Professor, Department of Civil Engineering, K. N. Toosi University of Technology, Tehran, Iran

Abstract

Eccentrically braced frames (EBF) are lateral resisting systems with appropriate ductility and strength against earthquakes. An important kind of arranging such systems, recommended by Popov and also presented in AISC, is eccentrically split-X bracing. The axial force applied to the beam outside link beam is reduced causing the improvement of the behaviour of this type of bracing. In this research, for the first time, ductility factor, overstrength factor and response modification factor of eccentrically split-X braces are investigated through nonlinear static and incremental dynamic analyses and fragility curves are presented for different ratios of link beam length to span length. For this purpose, three buildings, 2-, 6- and 10-storey structures with the ratios of link beam length to span length (e/L) of 0.05, 0.1, 0.15 and 0.2 are considered. Ductility factor of R_{μ}=3.55, overstrength factor of R_s = 2.31 and response modification factor of R_{LRFD} =8.06 are calculated under 10 earthquake records. It is concluded that the most appropriate values of *e/L* ratio in the eccentrically split-X bracing are 0.1 for tall structures and 0.05 for small ones. According to the log-normal distribution, the fragility curves are also plotted considering collapse prevention (CP) and immediate occupancy (IO) performance levels.

Keywords: Eccentrically split-X; Link beam; Incremental dynamic analysis; Response modification factor; Fragility curve.

1. Introduction

Todays, the systems resistant to earthquake-induced lateral forces are used in the buildings to withstand such forces. One of these systems is Eccentrically Braced Frames (EBF).
Several researches have been performed by the scientists of University of California at Berkeley on seismic behaviour of eccentrically braced frames in 1970-1990 [1-6], evaluating these systems in the real and scaled forms [7- 9]. The universities of Nevada [10, 11],

* Corresponding author. K. N. Toosi University of Technology, Civil Engineering Department, No. 1346, Vali-Asr Street, P.O. Box. 15875-4416, 19697 Tehran, Iran, Tel.: +98 21 8877 9623, Mobile No.:,E-mail address: fanaie@kntu.ac.ir (Nader Fanaie)

California [12] and Texas [13-16] have also conducted some experimental tests on the link beams.

The recent investigations performed by the researchers showed that EBFs can provide significant elastic stiffness, and most particularly in case of small link beam, comparing to SCBF (Special Concentrically Braced Frame) and OCBF (Ordinary Concentric Brace Frame) bracing systems. If the connection length is not too short, then ductility and energy dissipation capacity will be excellent in the inelastic deformation and comparable to SMRF (Steel Moment Resisting Frame).

Okazaki et al. at 2005 [17] studied steel link beams subjected to cyclic loading and assessed their performances through a sum of 23 tests. Chao et al. at 2006 [18] investigated the web failure, observed earlier in the experiments, using computational simulation.

Rossi and Lombardo in 2007 [19], studied the effects of overstrength factor on the seismic behaviour of eccentrically braced frames, designed according to the capacity based design method. Ozhendekci et al. in 2007 [20], performed numerical investigations to evaluate the effects of the geometry of eccentrically braced frames on their weights and inelastic behaviours. For this purpose, they designed 420 eccentrically braced frames with short link beams, 105 with medium link beams and 105 with long link beams.

Chegenia and Mohebkhah in 2014 [21] by examining the three long link beams that were modeled on ABAQUS, showed that, although the rotation in the long link beam was limited to 0.02, using mid stiffeners, provides the benefits of long link beams in terms of architecture.

Kurdi et al. in 2017 [22] conducted some experiments on the residual stresses of link beam and showed that the highest tensions occur in certain areas, called K. They showed that the effects of residual stress can be reduced using appropriate horizontal and vertical stiffeners and the link beam performance can be improved.

Ming in 2017 [23] by examining the eccentric brace with a vertical link beam, which was tested on two samples with a scale of 1 to 2, concluded that the structure weight is considerably reduced using a high-strength steel in beams and columns. They concluded that use of ordinary steel for link beams provides the necessary ductility for the structure and greatly affects the energy absorption.

Tian et al. in 2018 [24] examined the 3-storey building with K-shaped eccentric brace scaled 1 to 2 and concluded that the link beams were the weakest part of the lateral force system of the structure. Based on their research, using high-strength alloy (K-HSS-EBF) in the beam, can reduce the energy input to the structure greatly.

Bosco and Rossi [25] in 2008 studied the effects of overstrength factor on the design of eccentrically braced frames. Different bracing arrangements are used in EBF.

Brunesi et al. in 2016 [26] attempted to model connecting beam to a column in high-rise mega-braced frame-core buildings with zero length element in OpenSees and Bosco et al. in 2016 [27] investigated effect of fatigue wedding gusset plate of industrial liquid tank supporting structure with braced frame systems within the open source finite element platform OpenSees.

One of these arrangements has been recommended by Engelhardt and Popov and also presented in AISC, (ANSI/AISC 341-05) [28] Figure 1. Such arrangement results in the optimum design of link beam by reducing or eliminating its axial force. It is worth mentioning that the Split-X eccentrically braced frame investigated in this study has a significant difference compared to the common eccentrically chevron V and inverse V braced frames causing it to show a different behaviour. The reason behind this, is the decrease in axial force of the beam outside the link beam as well as the increase in shear force in the link beam of the Split-X eccentrically braced frames in comparison with the usual chevron braced

frame which is owing to different sign (tensile and compressive) of the upper and lower braces of the floor reckoned as a highly desirable phenomenon.

Because the axial force reduction of the outside link beam the in Split-X EBF causes the buckling potential to be diminished for this beam. Thus the length of it is not short the same as the link beam, and that is more important, shear force in the link beam of the Split-X EBF increases compared to the usual chevron braced frame in the same condition. resulting in the link beam of the Split-X eccentrically braced frame to have a more reliable shear behaviour compared to the conventional eccentric chevron braced one, and has a definitely shear failure mode. However, no considerable researches have been conducted on the mentioned EBF arrangement. So far, no investigation is found on the evaluation of response modification factor, ductility and overstrength factors of this system. This research focuses on the studying and obtaining the response modification factor, ductility and overstrength factors of such kind of bracing system arrangement, called split-x, using incremental dynamic analysis (IDA).

2. Eccentrically braced frame

The bracing and link beam are designed for appropriate seismic performance of EBF in such a way that under ultimate loading condition, yielding the link beam prevents the bracing from buckling. For ensuring, ultimate capacity of link beam is evaluated precisely and EBF is designed in such a way to occur inelastic deformation in the link beam under severe seismic loading. By the way, the link beams act as structural fuses which prevent the braces from buckling. Figure 2 presents the ordinary EBFs [18].

The important factor in controlling the behaviour of link beam is its length. Short link beams are yielded in the shear, long ones in the bending moment, and medium in the combination of shear and bending moment. The performance and energy absorption of short link beams are more appropriate comparing to those of medium and long ones. The following steps are considered in design of EBF systems [28]:

a) Estimating the shearing capacity needed for link beam and selecting the sections;
b) Designing other elements in such a way that structural fuse can be created in the link beam;
c) Estimating the demand ductility for the structure and determining the details necessary for the link beam.

3. Incremental Dynamic Analysis (IDA)

Random intrinsic nature of earthquakes is one of the main uncertainties in assessing the seismic behaviour of structures. For quantifying such uncertainty, the seismic response of structure should be determined performing different dynamic analyses in the course of different earthquake ground motion. In this study earthquake uncertainty has been considered using Incremental Dynamic Analysis (IDA). In this regard, sufficient numbers of records are used to consider the uncertainties in the frequency content and earthquakes records spectra shapes [29]. Then each earthquake record is scaled in such a way that can cover appropriate ranges of seismic intensities and also structural responses, from elastic limit to collapse. For IDA analysis, the intensity measure (IM) (eg: PGA (Peak ground acceleration) or $S_a\ (T_1)$) is scaled with a proper algorithm, starting from a very low amount to a certain level, in order to motivate the elastic response in the considered structural model and target collapse state respectively. Time history analysis is conducted in IDA, using different records generated by

various scale factors. At the end of each analysis, the DM (Damage Measure) values are determined, corresponding to the IM levels, used in dynamic analysis.

For utilizing IDA analysis, selecting appropriate parameters for IM and DM is of greatest significance. The mentioned parameters should be scalable in order to be selected for a suitable seismic intensity. In this study, the spectral acceleration of the first mode is chosen as IM to include the principal period of structure in the scaling and consider the earthquake duration and damping parameters. Joint rotation, inter-storey drift, roof displacement and axial deformation of elements can be used as the collapse criteria of structures. In this research, maximum inter-storey drift is considered as DM to achieve appropriate structural response against earthquake records.

4. Calculating the seismic parameters of structure

Response modification factor is considered in almost all universal codes for reducing the calculated earthquake loads in order to consider inelastic behaviour. This allows the designers to conduct elastic analysis under reduced loads and designing the structures based on the obtained results. The mentioned factor depends on different aspects, the most important of which are: ductility of structure, material properties, damping characteristics, cooperation of non- structural members, overstrength etc.

In this study, response modification factor is calculated using Uang's ductility factor method [30] in which real nonlinear behaviour is usually idealized by a bilinear elasto perfectly plastic relation, (Figure 3), [31].

In order to calculate response modification factor, some parameters are defined using the base shears shown in Figure 3. The first type is overstrength factor. The overstrength phenomenon is important in earthquake occurrence and each frame presents different overstrength under different earthquakes. Overstrength factor is calculated through IDA in this research. Here, the method that is presented by Mwafy & Elnashai [32], is used for computing maximum base shear through IDA. Thus, this involves a structural model subjected to one (or more) ground motion record(s), each of which is scaled to multiple intensity levels [33]. Overstrength factor is expressed in Equation (1):

$$R_s = \frac{V_{b(Dyn,u)}}{V_{b(st,y)}} \tag{1}$$

It means that overstrength is the ratio of dynamic base shear obtained from mechanism formation and collapse in the structure to the static base shear corresponded to the first plastic hinge formation. Overstrength factor considers the actual lateral strength of structure against its design lateral strength.

In the method presented by Mwafy & Elnashai [33], the ductility factor is obtained directly, as well as, by using the results of IDA and linear dynamic analysis as Equation (2):

$$R_\mu = \frac{V_{b(Dyn,el)}}{V_{b(Dyn,u)}} \tag{2}$$

In order to obtain $V_{b(Dyn,u)}$, the spectral acceleration of earthquake record (the intensity measure applied in this study) increases up to form mechanism in the structure or meet the considered damage. Basically, such spectral acceleration, which leads to the above mentioned mechanism or damages, is accepted as ultimate limit where the corresponded base shear is obtained. Additionally, maximum linear base shear of the structure is also calculated through dynamic analysis, assuming elastic behaviour of structure under the same spectral

acceleration. The base shear, corresponded to the first plastic hinge, which has been obtained through nonlinear static analysis, is used for calculating the overstrength factor. It means that the end of linear zone, corresponded to the first plastic hinge, can be considered the same in both static and dynamic analyses [32]. Ductility factor depends on several aspects including the type of structural system, the quality of connections, number of stories, etc.

Allowable stress factor (Y) Equation (3): in the designing codes, V_s is reduced to V_w through a factor called allowable stress factor, the amount of which is considered as 1.44 in this research [30].

$$Y = \frac{V_s}{V_w} \tag{3}$$

In fact the origin of response modification factor is strength reduction factor due to ductility (R_μ) and overstrength factor (R_s). These two factors have already been defined.

Response modification factor with ultimate strength method is defined as Equation (4):

$$R_u = \frac{V_e}{V_y} \times \frac{V_y}{V_s} = R_\mu \times R_s \tag{4}$$

Response modification factor with allowable stress design method is expressed as Equation (5):

$$R_w = \frac{V_e}{V_y} \times \frac{V_y}{V_s} \times \frac{V_s}{V_w} = R_\mu \times R_s \times Y \tag{5}$$

5. IDA analyses

For performing IDA, several earthquake records should be selected properly. Regarding the soil type, the stations of these records should be similar to the site in which the structure is located. In this regard, 10 records of the world well-known earthquakes are chosen and presented in Table 1. Shear wave velocities of the stations are in accordance with those of the soil type II in Iranian standard No. 2800.

An appropriate algorithm should be used for scaling the seismic intensity to optimize the scaling numbers of each record for analyzing and have the sufficient accuracy and velocity for meeting the scale of seismic intensity which causes the failure of structure. For this purpose, hunt and fill algorithm has been used in the present research. In this method, for scaling the seismic intensity, first, a very low value (0.005g) is selected for seismic intensity parameter (spectral acceleration of the first mode) which guarantees the linear response of structure. Then, in the searching step, for finding the range of spectral acceleration of the first mode in which the considered failure has been occurred, the seismic intensity increases in each step, based on the below formula, using the least numbers of points. Therefore, the value of $S_a\ (T_1)$ in each step is equal to value of $S_a\ (T_1)$ in the previous step plus α times the number of its previous step (Equation (6)). In this study α is considered 0.05.

$$S_a(T_1)_i = S_a(T_1)_{i-1} + \alpha \times (i-1) \tag{6}$$

6. The studied models

In this research, 12 eccentrically split-X braced frames are investigated tri-dimensionally, including 2-, 6- and 10-storey structures with the ratios of link beam length to span length (*e/L*) of 0.05, 0.1, 0.15 and 0.2. It is assumed that they are located in the San Francisco in California (very high relatively seismic region) on soil type D, according to ASCE-7-10. [34]
Regarding the initial response modification factor of R_{LRFD}=7.5, the structural components (bracings, beams and columns) is firstly designed. This design results in act the link beam as a structural fuse. Then response modification factor has been calculated as 8 using the results of push over analysis based on adaptive push over and this factor is used for designing the main structures.
The structures are designed and analyzed using ETABS Nonlinear v13.1.1 software, which considers AISC 360-10 code for designing the elements. The applied steel is A992Fy50, the height of all stories 3.2m, span lengths 6m, dead load 400 kg/m^2 and live load 200 kg/m^2.
The distribution of lateral force used in this research is based on the first mode of the structure and inverted triangle. In the analysis, it is assumed that a vibration mode dominates the behaviour of the whole structure and the corresponding mode shape remains constant during the analysis. This kind of force distribution is used according to the Iranian code for nonlinear static analysis.
All the connections between beam to column as well as the braces to each other are hinge forms on the frame plane. The plans of all stories are considered the same in the studied structures. Figure 4 presents the plan and the locations of braces, in dotted lines. Figure 5 shows the configuration of the frames extracted from tri-dimensional structure. Plate girder has been used for link beams of braced spans for controlling the unbalanced tension and compression axial forces. Tables 2-5 present the properties of structural components in the studied frames.

7. Modeling in the OpenSees software

In this research OpenSees [35] software has been used for modeling and performing nonlinear static and time history dynamic analyses. This software, produced by University of California, Berkeley, is one of the strongest software for nonlinear and dynamic analyses using fiber elements. Nonlinear beam column element with controlling the displacement has been used to model the columns, bracings and beams in this software.
This element can take into account the effects of P- delta and large deformations for considering the geometric nonlinear effects. In order to model the distributed plasticity of elements in OpenSees program, the sections of each element (beams, columns and bracings) are divided into several fibers (120 fibers for flange and web cross sections). These elements are divided into several segments in their lengths as well. Moreover, steel materials are modeled using uniaxial material hysteretic behaviour model which can model the behaviour of steel in tri-linear forms in compression and tension. By this behaviour curve, the points of yielding, failure and buckling of each element can be presented to the program. The slope of strain hardening of steel in tension has also been considered as 2% of the slope of elastic region. Also for modeling of damping, Rayleigh damping is used in which the parameters α and β are calculated based on the period of each structure. For geometric transformation, P-delta transformation command is used for braces and columns and Corotational command for beams. Zero-length element has been used in the connection of beam to column as well as bracing to beam and column for modeling hinge connections of the frame elements. The nodes are constrained in the hinge connection location only in the degrees of

freedom of translation. The storey's mass is considered as lumped mass in the nodes and storey's floors as rigid diaphragm.

Shear behaviour of the link beam has been modeled according to Rozon et al. research, considering parallel material and zero length element [36].

For validation of nonlinear behaviour of link beam due to dynamic analysis, the Okazaki model [17] has been used, which has examined hysteresis behaviour of the link beam.
Figure 6 compares the results of finite element modeling and experimental test on the link beam.

The Okazaki experimental study included 12 specimens in which *W10x33* section (with length of 584 mm) was used for verifying. The alloy used at this section is ASTM A992 (F_y= 345 MPa). According to Bosco et al. research [27], a zero-length element has been used to model the shear behaviour of link beam in the OpenSees software, based on the shear capacity of each cross section. Figure 7 shows how this experiment is conducted.

8. The results of analysis

8.1. Nonlinear static analysis

Adaptive push over analysis is used for obtaining the base shear force using nonlinear static analysis. According to the structural failure criteria in ASCE, when the structure meets these criteria, the base shear force is recorded which is used for calculating the response modification factor of structure .
Figures 8-10 present the push over curves of structure for triangular lateral load pattern.

These figures show that with increasing the number of stories, the ratio of e/L has more effect on structure stiffness and when this ratio increases, the stiffness of structure is reduced in 10-storey so faster than 2- and 6-storey.

8.2. Incremental Dynamic Analysis (IDA)

Figures 11-22 present IDA curves for the studied frames. All behaviour steps of the structure under earthquake are evident in the curves (from elastic limit to collapse limit).

According to the curves, in general with increasing the heights of structures, the structures enter the nonlinear region sooner. Moreover, IM values are reduced in the curves for a constant value of *DM*. In the other words, it can be said that S_a corresponded to a certain damage criterion, is reduced with increasing the height of structure.

8.3. Calculating response modification factor

Tables 6-17 present ductility, overstrength and response modification factors of the studied frames for ultimate state and allowable stress design methods, considering the results obtained from nonlinear static and nonlinear time history dynamic analyses for the selected records as well as the explanations presented in section 3 of this research.

The values of overstrength, ductility and response modification factors for 2, 6 and 10-storey frames are summarized and presented in Table 18 versus the ratio of link beam

length to the span length. Ductility factor, overstrength factor and response modification factor of 2, 6 and 10-storey structures are presented in Figures 23-25, respectively.

Considering the curves, plotted for 10-storey structure, the ductility factors are higher for each ratios of *e/L*, comparing to those of overstrength factors. Moreover, the differences between the values of these parameters are reduced with decreasing the stories. In the 2-storey structure, the mentioned difference is observed in most of the ratios excluding *e/L*=0.05. Therefore, the higher effect of ductility, comparing to that of overstrength, is more significant in the tall structures in comparison with that of short ones.

Regarding the response modification factor, the proper value of link beam length to span length ratio (*e/L*) is 0.1 in 6- and 10-storey structures. However, this value (*e/L*) is 0.05 in the 2-storey structure due to the high value of overstrength factor in this ratio which results higher response modification factor. Therefore, better seismic behaviour for this kind of bracing is achieved using *e/L* of 0.05 in small structures and e/L of 0.1 in tall structures.

9. Fragility curves

In order to better investigate the behaviour of considered braces, the fragility curves are plotted according to log normal distribution, evaluating the damage probability of structures under different acceleration spectra. The fragility curves are mostly modeled by cumulative log normal functions, presenting the occurrence probability or exceeding a damage status for certain intensity scale of earthquake [37-39]. In this research, the fragility curves are plotted according to the spectral acceleration in the period of structures, modeled in the form of two parameters lognormal function. The occurrence probability of damage status (D_{Si}) is obtained in a certain spectral acceleration, $S_a(T1,g)$, as Equation (7) [40] :

$$P(DS \geq D_{si} \mid S_a(T_1)) = \phi\left(\frac{\ln x - \lambda}{\beta}\right) \quad (7)$$

where, ϕ is the standard accumulative lognormal distribution function; x is the spectral acceleration with lognormal distribution; and λ and β are average and standard deviation of ln x. Damage criterion has been considered for the structures, presented in Table C1-3, based on the drift values and according to ASCE (41-06) [41] guideline as 2% for collapse prevention and 0.5% for immediate occupancy. Figures 26-28 present the fragility curves for each structure for performance levels of immediate occupancy (*IO*) and collapse prevention (*CP*) in different ratios of link beam length to span length.

Considering the fragility curves in the performance level of immediate occupancy, the values of spectral acceleration are reduced with increasing the heights of structures. Moreover, with increasing *e/L* ratio in a structure with constant storeys, lower spectral acceleration causes its damage curves in performance level of immediate occupancy.

The extension is observed in all fragility curves plotted for performance level of collapse prevention, indicating the effects of the contents of applied earthquakes for creating the considered damage. This extension is lower for the performance level of immediate occupancy. Regarding the fragility curves, 2-storey structure with *e/L*=0.05 presents the best seismic behaviour in the models with different *e/L* ratios. However, *e/L*=0.1 is the appropriate ratio in the 6- and 10-storey structures.

10. Discussion on the results

As incremental dynamic analysis is time and high energy consuming, it is not possible to consider as many models for investigating the effects of ratio of link beam length to span

length as well as the height of structure on seismic behaviour of eccentrically split-X braced frames.

In this research, 12 models are studied with different heights and link beam length to span length ratios. Based on the obtained results, the stiffness of structures is reduced with increasing the length of link beam. The reason is that the angle between the bracing and horizontal direction increases in the structure with longer link beam; and therefore the stiffness of bracing decreases against lateral loads. The structure presents more ductility with the increase of *e/L* ratio values. As fundamental period of structure increases with decreasing its stiffness, the probability of the resonance phenomenon formation is reduced and IDA curves become more regular. The values of response modification factor are reduced with the increase of the heights of structures. The reason is the decrease of ductility factor due to more softening of structures with increasing their heights.

Under a constant spectral acceleration, damage probability of structure increases with the increase of *e/L* ratio as well as the reduction of its height, due to higher flexibility of structure. Response modification factor is calculated through multiplying overstrength factor by ductility factor. In 6- and 10-storey structures these two parameters have optimum values in *e/L*=0.1 due to the proper stiffness and ductility in this ratio. However, in the 2-storey structure, *e/L*=0.05 is the best because of high overstrength factor in this ratio. The reason of this phenomenon is the resistance of structure with low periods against the applied records. That is, the spectral acceleration needed for such structures to reach the damage level is higher than the spectral acceleration of other structures with high periods.

11. Conclusions

The results obtained from analyses are briefly summarized as follows:

1. Considering pushover analysis curves, all structures become more flexible with the increase of *e/L* ratio values. This stiffness reduction is more obvious in the 10-storey structure.
2. The IDA curves become more regular with lower dispersion by increasing the ratio of link beam length to span length.
3. Mean values obtained for response modification factor (corresponding to ultimate limit state), ductility and overstrength factors are 8.06, 3.55 and 2.31, respectively.
4. The values of response modification factor are reduced with increasing the height of structure.
5. The most appropriate values of *e/L* ratio in the eccentrically split-X bracing are 0.1 for tall structures and 0.05 for small ones.
6. The damage probability increases in a constant spectral acceleration with increasing the ratio of link beam length to span length.
7. The spectral acceleration needed for creating target displacement is reduced in IDA curves with increasing the height of structure.

References

[1] Roeder, C.W. and Popov, E.P. “Inelastic behaviour of eccentrically braced steel frames under cyclic loadings”. Report no. UCB/EERC-77/18. Berkeley (CA): Earthquake Engineering Research Center (1977).

[2] Hjelmstad, K.D. and Popov, E.P. “Seismic behaviour of active beam links in eccentrically braced frames”. Report no. UCB/EERC-83/15. Berkeley (CA): Earthquake Engineering Research Institute (1983).

[3] Malley, JO. and Popov, EP. “Design considerations for shear links in eccentrically braced frames. Report no. UCB/EERC-83/24. Berkeley (CA): Earthquake Engineering Research Institute (1983).

[4] Kasai, K. and Popov, EP. “A study of seismically resistant eccentrically braced frame systems”. Report no. UCB/EERC-86/01. Berkeley (CA): Earthquake Engineering Research Institute (1986).

[5] Ricles, JM and Popov, EP. “Experiments on eccentrically braced frames with composite floors”. Report no. UCB/EERC-87/06. Berkeley (CA): Earthquake Engineering Research Institute (1987).

[6] Engelhardt, MD and Popov, EP. “Behaviour of long links in eccentrically braced frames”. Report no. UCB/EERC-89/01. Berkeley (CA): Earthquake Engineering Research Institute (1989).

[7] Foutch, D. A., Goel, S. and Roeder, C. W. "Seismic testing of full-scale steel building, part I.", Journal of Structural Engineering, ASCE, 113 (11), pp. 2111-2129 (1987).

[8] Roeder, C.W., Foutch D.A. and Goel S.C. “Seismic testing of full-scale steel building, part II”, Journal of Structural Engineering, ASCE; 113 (11): 21936 (1987).

[9] Whittaker, A.S., Uang, C.M. and Bertero, V.V. “Earthquake simulation tests and associated studies of a 0.3-scale model of a six-story eccentrically braced steel structure”. Report no. UCB/EERC-87/02. Berkeley (CA): Earthquake Engineering Research Center, University of California (1987).

[10] Itani, AM. “Cyclic behaviour of Richmond-San Rafael tower links”, Report no. CCEER 97-4. Reno (NV): Center for Civil Engineering Earthquake Research, University of Nevada at Reno (1997)

[11] Dusicka, P. “Built-up shear links as energy dissipators for seismic protection of bridges”. Ph.D. dissertation. Reno (NV): Department of Civil and Environmental Engineering, University of Nevada (2004).

[12] McDaniel, C. C. , Uang, C.M. and Seible, F. "Cyclic testing of suspension tower shear links of the San Francisco (CA)" Department of Structural Engineering, University of California (2002).

[13] Arce, G. “Impact of higher strength steels on local buckling and overstrength of links in eccentrically braced frames”, M.S. thesis. Austin (TX): Department of Civil, Architectural and Environmental Engineering, The University of Texas at Austin (2002).

[14] Galvez, P. “Investigation of factors affecting web fractures in shear links”, M.S. thesis. Austin (TX): Department of Civil, Architectural and Environmental Engineering, The University of Texas at Austin (2004).

[15] Ryu, H.C. “Effects of loading history on the behaviour of links in seismic-resistant eccentrically braced frames”, M.S. thesis. Austin (TX): Department of Civil, Architectural and Environmental Engineering, The University of Texas at Austin (2005).

[16] Okazaki, T. “Seismic performance of link-to-column connections in steel eccentrically braced frames”, Ph.D. dissertation. Austin (TX): Department of Civil, Architectural and Environmental Engineering, The University of Texas at Austin (2004).

[17] Okazaki, T., Arec, G., Ryu, H.C. and Engelhardt, M.D. “Experimental Study of Local Buckling, Overstrength and Fracture of Links in Eccentrically Braced Frames”, Journal of Structural Engineering, (2005).

[18] Chao, S.H., Khandelwal, K. and Sherif, E.T. “Ductile Web Fracture Initiation in Steel Shear Links”, Journal of Structural Engineering, (2006).

[19] Rossi, P.P. and Lombardo, A. “Influence of Link Overstrength Factor on Seismic Behaviour of Eccentrically Braced Frame”, Journal of Structural Engineering, 63(11), pp. 1529-1545 (2007).

[20] Ozhendekci D. and Ozhendekci N. “Effects of the Frame Geometry on the Weight and Inelastic Behaviour of Eccentrically Braced Chevron Steel Frames”, Journal of Constructional Steel Research, 64(3), pp. 326-343 (2008).

[21] Chegeni, B. and Mohebkhah, A. “Rotation capacity improvement of long link beams in Eccentrically Braced Frames”, Scientia Iranica, 21(3), pp. 516-524 (2014).

[22] Kurdi, K., Budiono, B., Moestopo, M., Kusumastuti, D. and Refai Muslih, M. “Residual stress effect on link element of eccentrically braced frame”, Journal of Constructional Steel Research, 128(1), pp 397-404 (2017).

[23] Ming L. and Mingzhou S. “Seismic performance of high-strength steel fabricated eccentrically braced frame with vertical shear link”, Journal of Constructional Steel Research, 137(10), pp. 262-285 (2017).

[24] Tian, X., Su, M., Lian, M., Wang, F. and Li,S. “Seismic behavior of K-shaped eccentrically braced frames with high-strength steel, Shaking table testing and FEM analysis”, Journal of Constructional Steel Research, 143(4), pp 250-263 (2018).

[25] Bosco, M. and Rossi, PP. “Seismic Behaviour of Eccentrically Braced Frames”, Engineering Structures, 31(3), pp. 664-674 (2008).

[26] Brunesi, E., Nascimbene, R. and Casagrande, L. “Seismic analysis of high-rise mega-braced frame-core buildings”, Engineering Structures, 115, pp. 1-17 (2016).

[27] Bosco, M., Marino, E.M. and Rossi, P.P. “Influence of modelling of steel link beams on the seismic response of EBFs” Engineering Structures, 127, pp. 459-474 (2016).

[28] AISC, Seismic provisions for structural steel buildings (ANSI/AISC 341-05).Chicago (IL): American Institute of Steel Construction, Inc, (2005).

[29] Vamvatsikos, D. and Cornell, C.A, “The Incremental Dynamic Analysis and Its Application to Performance-Based Earthquake Engineering”, 12th European Conference on Earthquake Engineering, pp 479. (2002).

[30] Uang, CM. “Establishing R (or Rw) and Cd factor for building seismic provision”, Journal of Structure Engineering, 117(1), pp. 19-28 (1991).

[31] Zahrai, S.M. and Jalali, M. “Experimental and analytical investigations on seismic behavior of ductile steel knee braced frames”, Steel and Composite Structures, Journal 16(1), pp. 1-21 (2014).

[32] Mwafy, A.M. and Elnashai, A.S. “Calibration of force reduction factors of RC buildings”, Journal of Earthquake Engineering, 6(22), pp. 239-273 (2002).

[33] Vamvatsikos, D. and Cornell, C.A. "Incremental Dynamic Analysis", Earthquake Engineering and Structural Dynamics, 31(3), pp. 491-514 (2003).

[34] ASCE/SEI 7-10. Minimum design loads for buildings and other structures. Reston, Virginia: American Society of Civil Engineers (ASCE), (2010).

[35] OpenSees Command Language, Incremental Dynamic Analysis, Earthquake Engineering, http://opensees.berkeley.edu/ (2003).

[36] Rozon, J., Koboevic, S. and Tremblay, R. "Study of Behaviour of Eccentrically Braced Frames in Response to Seismic Loads", The 14th World Conference on Earthquake Engineering, October 12-17, Beijing, China (2008).

[37] Gulec, C.K., Gibbons, B., Chen, A. and Whittaker, A.S. "Damage states and fragility functions for link beams in eccentrically braced frames". Journal of Constructional Steel Research 67(9), pp. 1299–309 (2011).

[38] Jalayer, F. and Cornell, C.A. "A Technical Framework for Probability-Based Demand and Capacity Factor Design", Pacific Earthquake Engineering Research Center PEER Rep. 2003/8, PEER Berkeley, Calif. (2003)

[39] Ellingwood, B.R. and Tekie, P.B. "Seismic fragility assessment of concrete gravity dams", Earthquake Engineering and Structural Dynamics, 32(14), pp. 2221-2240 (2003).

[40] Wen, Y.K., Ellingwood, B.R. and Bracci, J. "Vulnerability Function Framework for Consequence-based Engineering", MAE Center Project DS-4 Report, April 28, 44. (2004).

[41] ASCE, American Society of Civil Engineers, Seismic Rehabilitation of Existing Buildings, ASCE/SEI 41-06.

Biographies

Nader Fanaie obtained his BS, MS and PhD degrees in Civil engineering from the Department of Civil Engineering at Sharif University of Technology, Tehran, Iran. He graduated in 2008 and, at present, is a faculty member of K. N. Toosi University of Technology, Tehran, Iran. He has supervised 30 MS theses up to now. His field of research includes seismic hazard analysis, earthquake simulation, seismic design and IDA. He has published 52 journal and conference papers, and also 10 books. He received 3rd place in the first mathematical competition, held at Sharif University ot Technology, in 1996, and a Gold Medal in "The 4th Iranian Civil Engineering Scientific Olympiad" in 1999. In 2001, he achieved the first rank in the exam of PhD scholarship abroad. He has also been acknowledged as an innovative engineer on 'Engineering Day', in 2008.

Ramin Sheykhi received her BS and MS degrees in Civil engineering respectively from the Department of Civil Engineering at University of Mohaghegh Ardabili, Ardebil, Iran and K. N. Toosi University of Technology, Tehran, Iran. He graduated in 2016, February. His field of research includes EBF seismic behaviour, Incremental Dynamic Analysis, Steel Structures and Fragility Curves.

Figure captions:

Figure 1: The arrangement of 2-storey eccentrically Split-X bracing (ANSI/AISC 341-05) [28]

Figure 2: Ordinary EBFs [18]

Figure 3: Elastic and inelastic responses of structure [30]

Figure 4: Plan of the studied structures

Figure 5: The configuration of studied structures

Figure 6 Comparison of the results of finite element modeling of link beam and Okazaki experimental test [17]

Figure 7: Details of Okazaki experimental test [17]

Figure 8: Pushover curves of 2-storey frame

Figure 9: Pushover curves of 6-storey frame

Figure 10: Pushover curves of 10-storey frame

Figure 11: IDA curves for 2-storey structure with e/L = 0.05

Figure 12: IDA curves for 2-storey structure with e/L = 0.1

Figure 13: IDA curves for 2-storey structure with e/L = 0.15

Figure 14: IDA curves for 2-storey structure with e/L = 0.2

Figure 15: IDA curves for 6-storey structure with e/L = 0.05

Figure 16: IDA curves for 6-storey structure with e/L = 0.1

Figure 17: IDA curves for 6-storey structure with e/L = 0.15

Figure 18: IDA curves for 6-storey structure with e/L = 0.2

Table captions:

Table 15: The values of overstrength, ductility and response modification factors for 10-storey frame with e/L = 0.15

Table 16: The values of overstrength, ductility and response modification factors for 10-storey frame with e/L = 0.1

Table 17: The values of overstrength, ductility and response modification factors for 10-storey frame with e/L = 0.05

Table 18: Mean values of overstrength, ductility and response modification factors for different frames

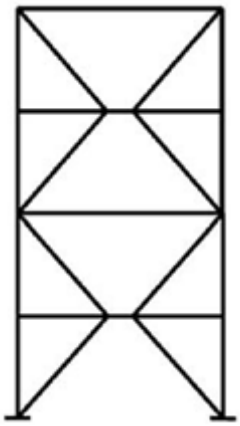

Figure 1

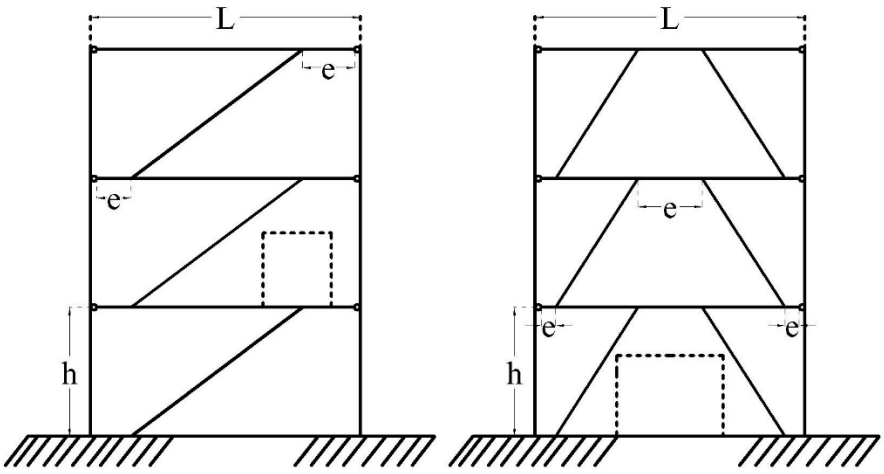

Figure 2

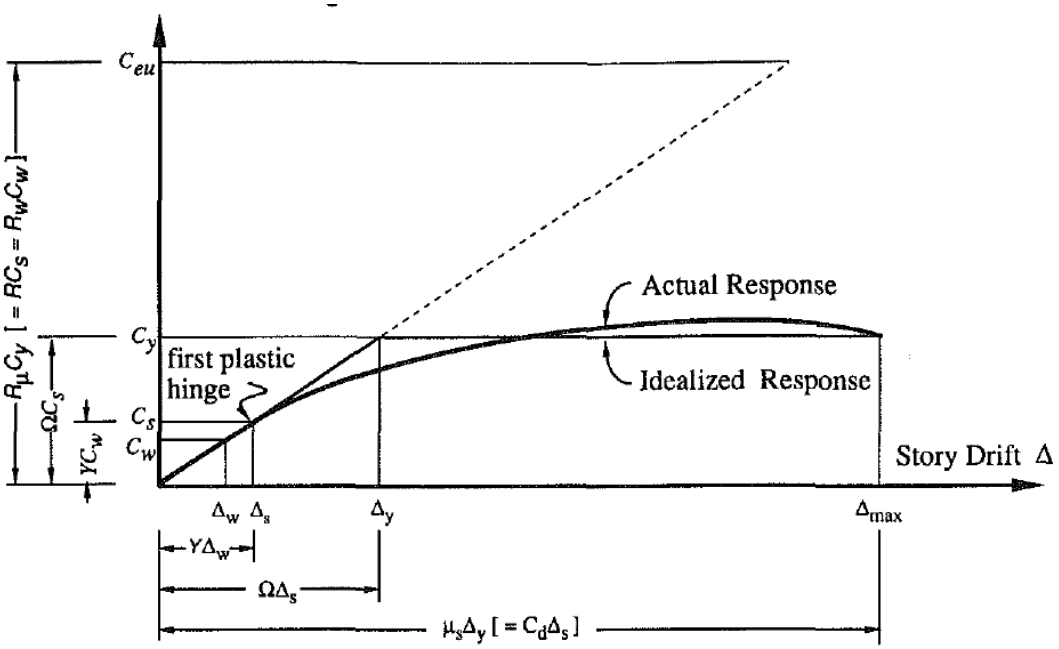

Figure 3

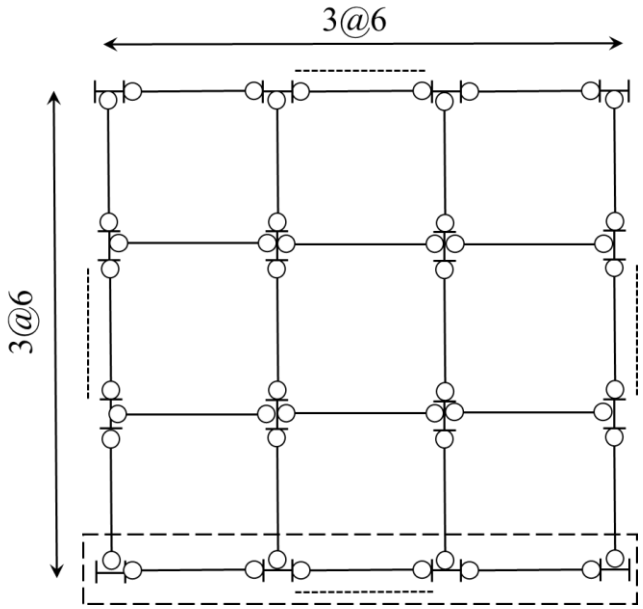

Figure 4

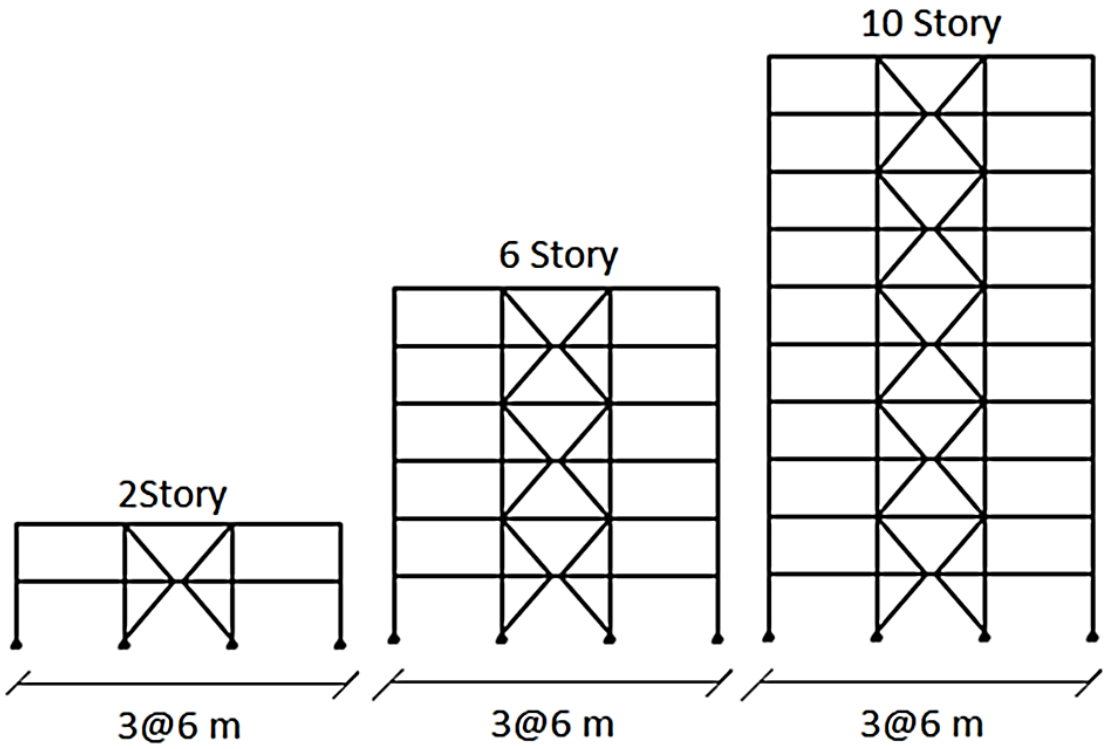

Figure 5

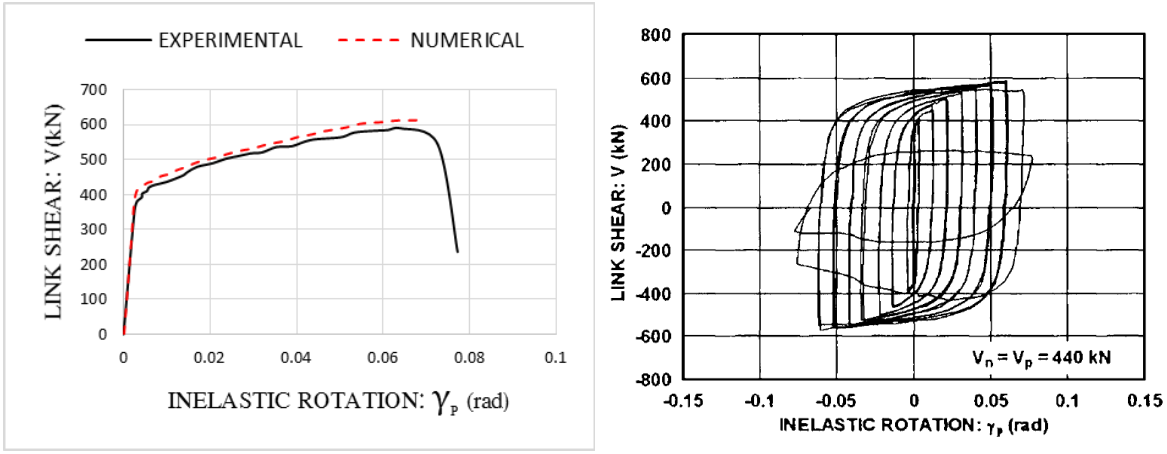

Figure 6

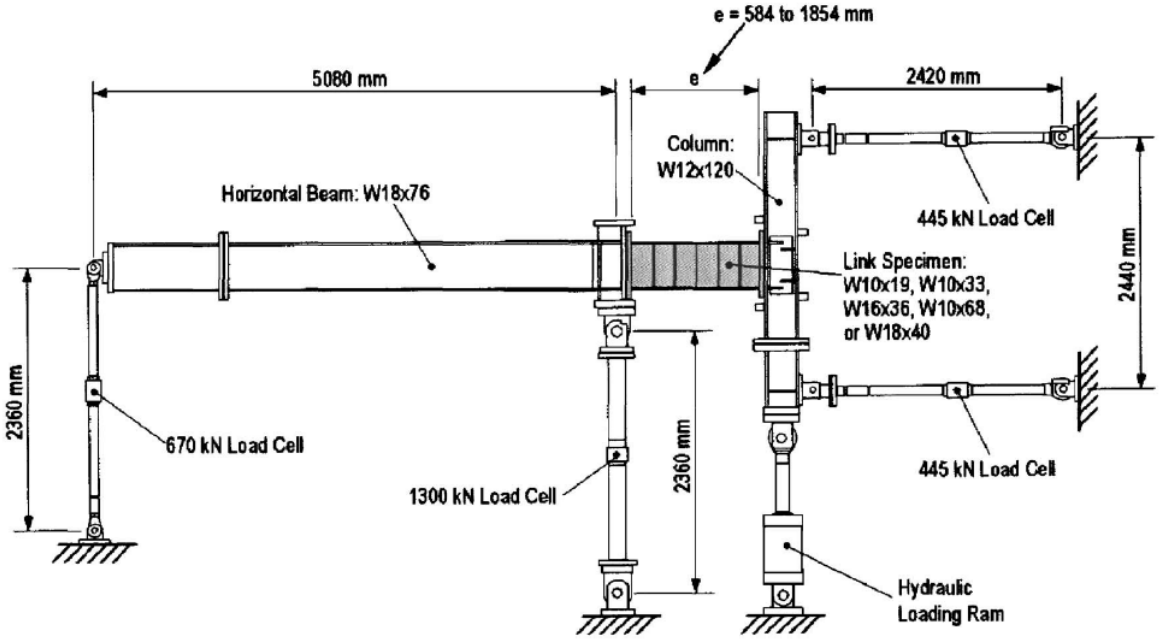

Figure 7

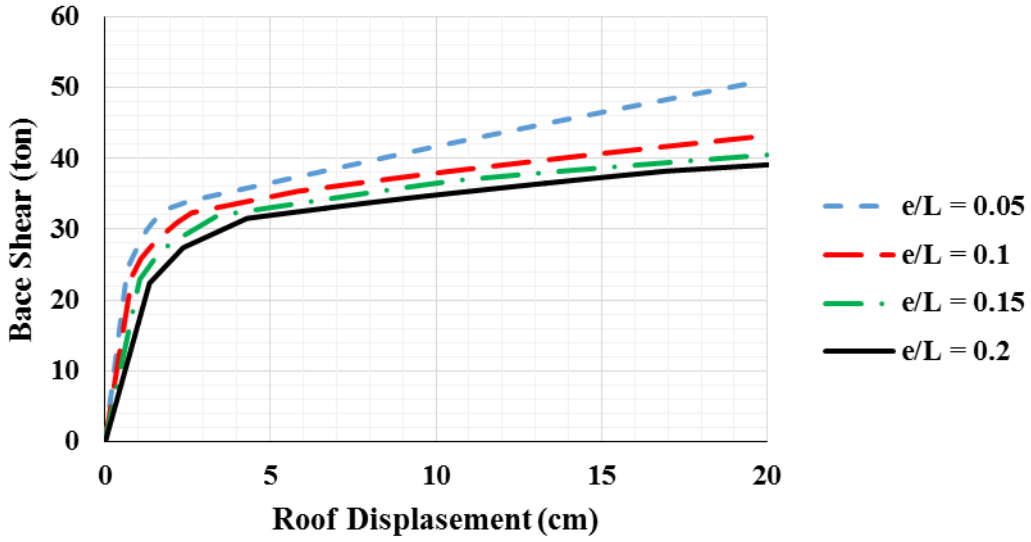

Figure 8

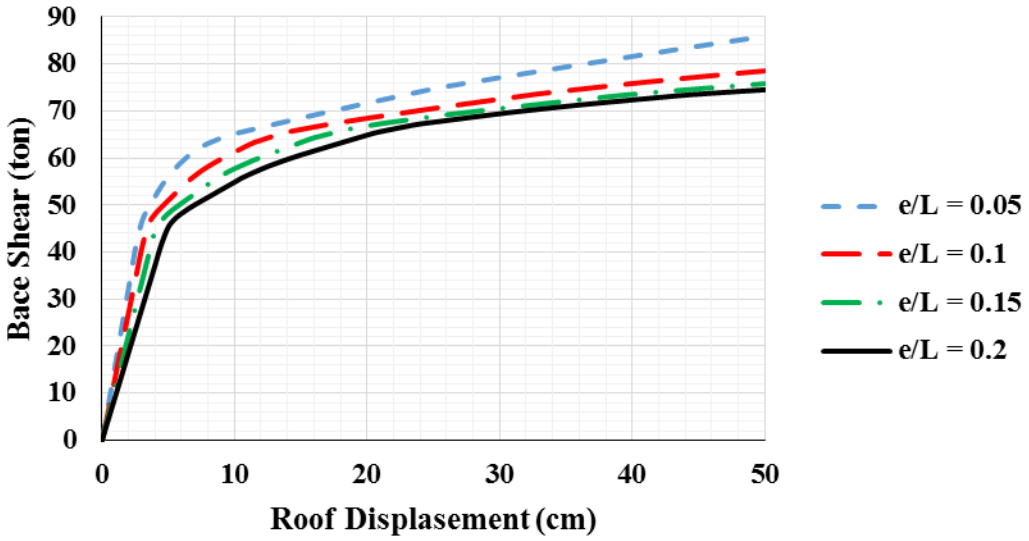

Figure 9

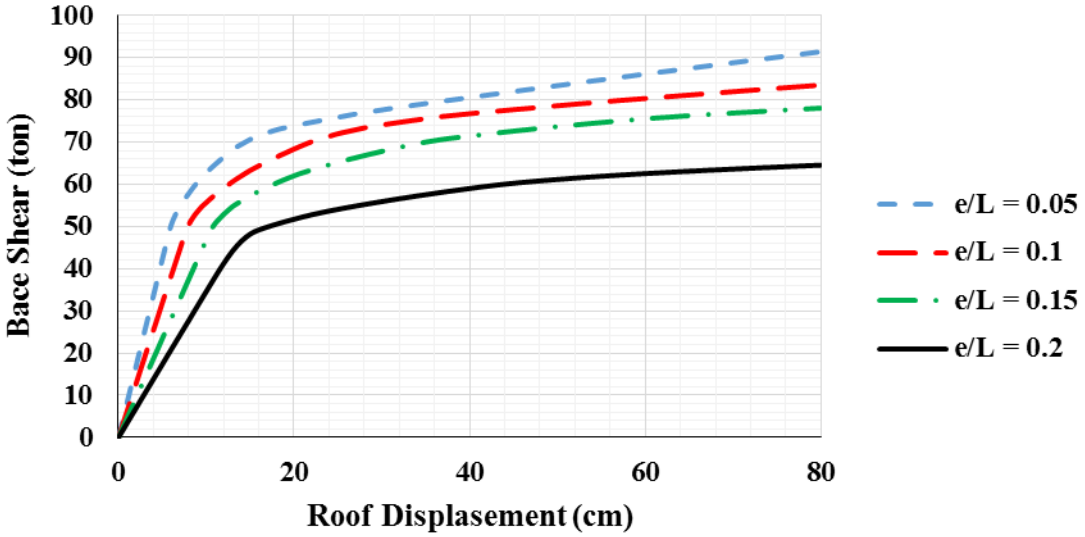

Figure 10

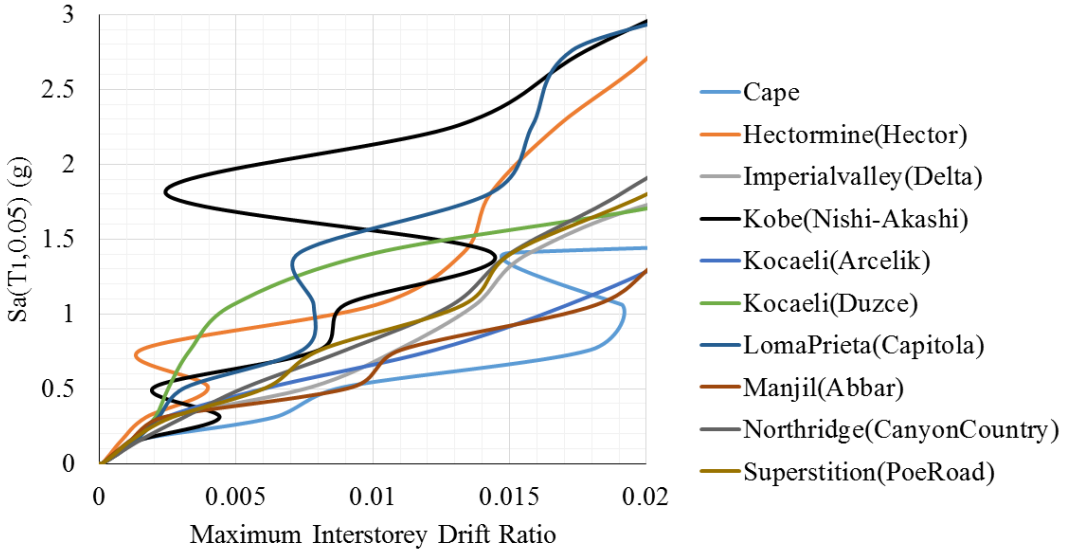

Figure 11

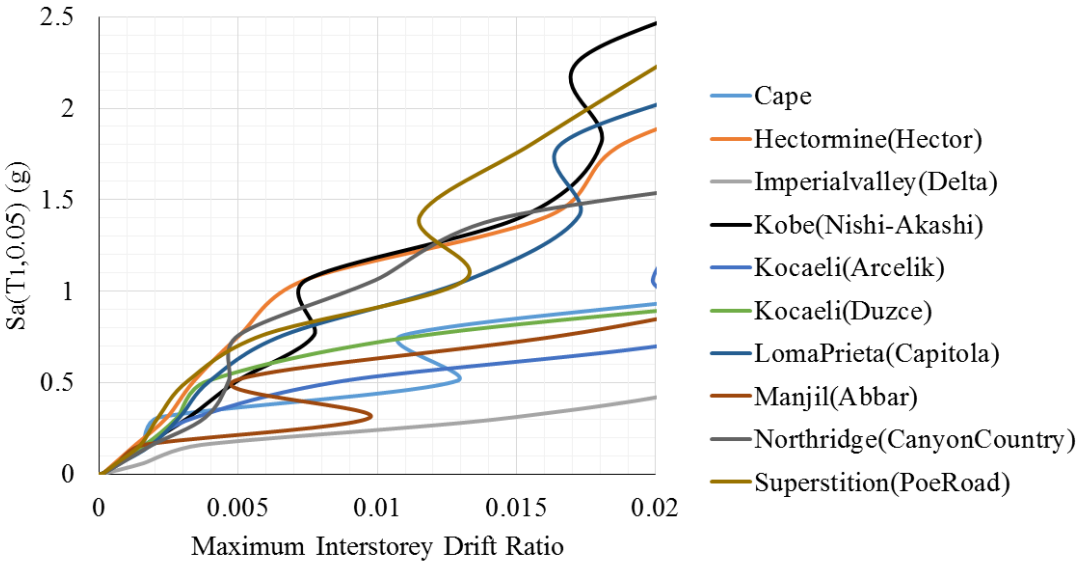

Figure 12

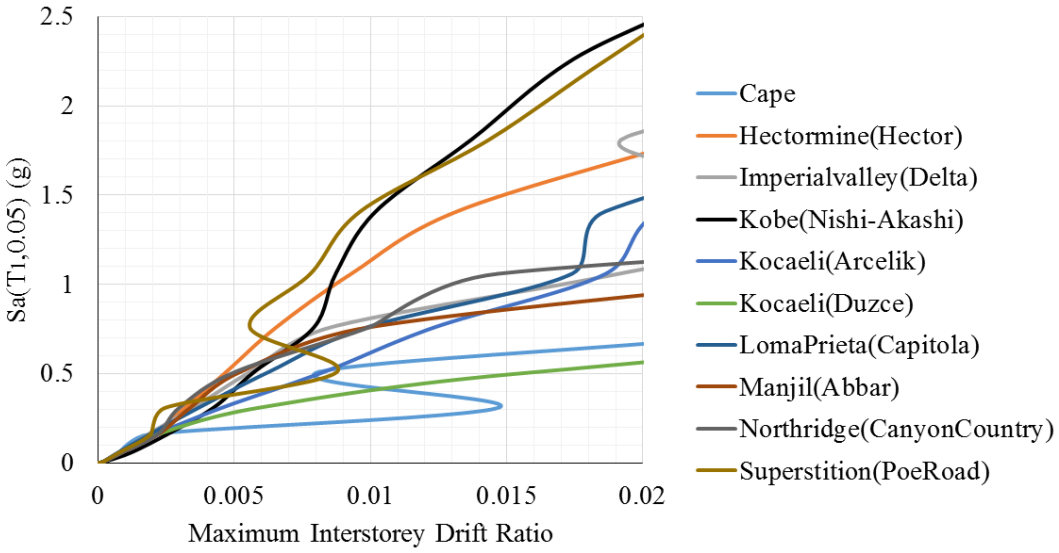

Figure 13

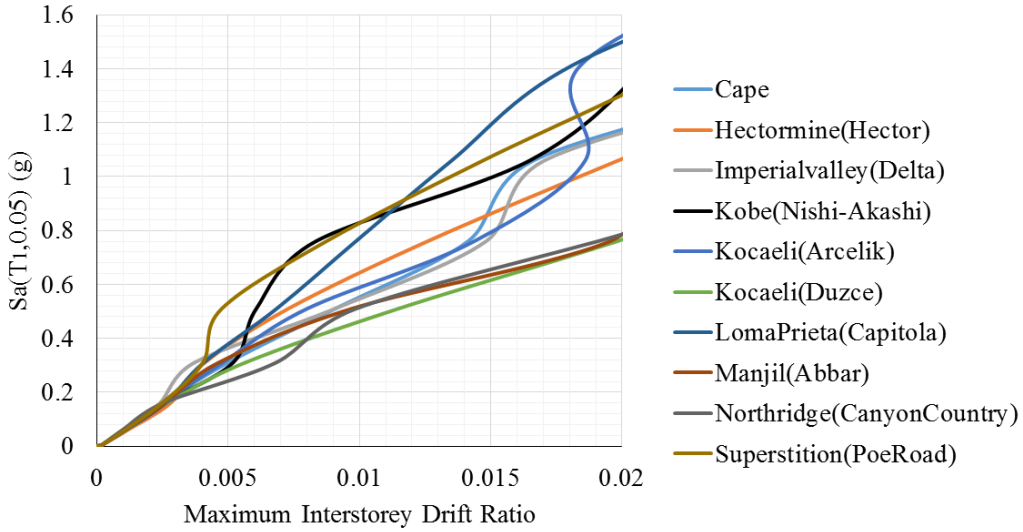

Figure 14

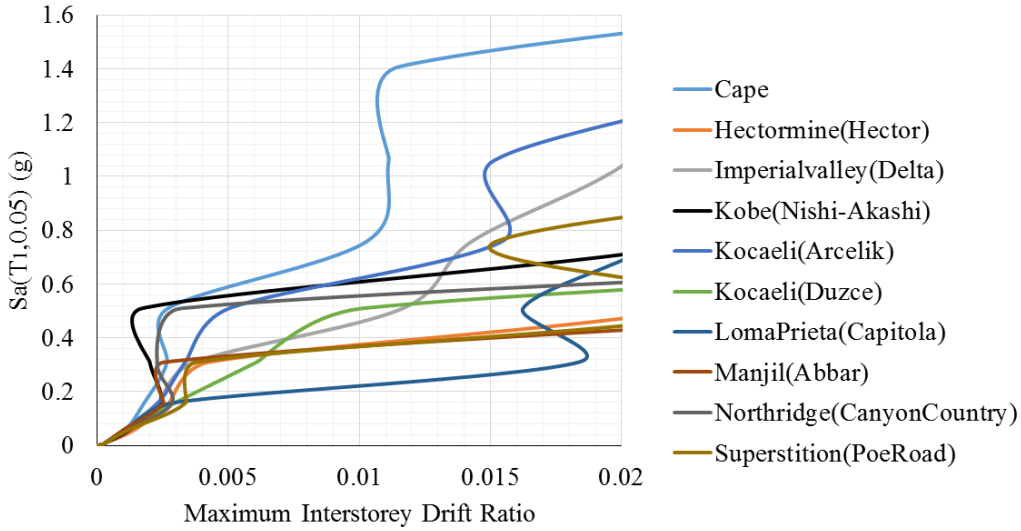

Figure 15

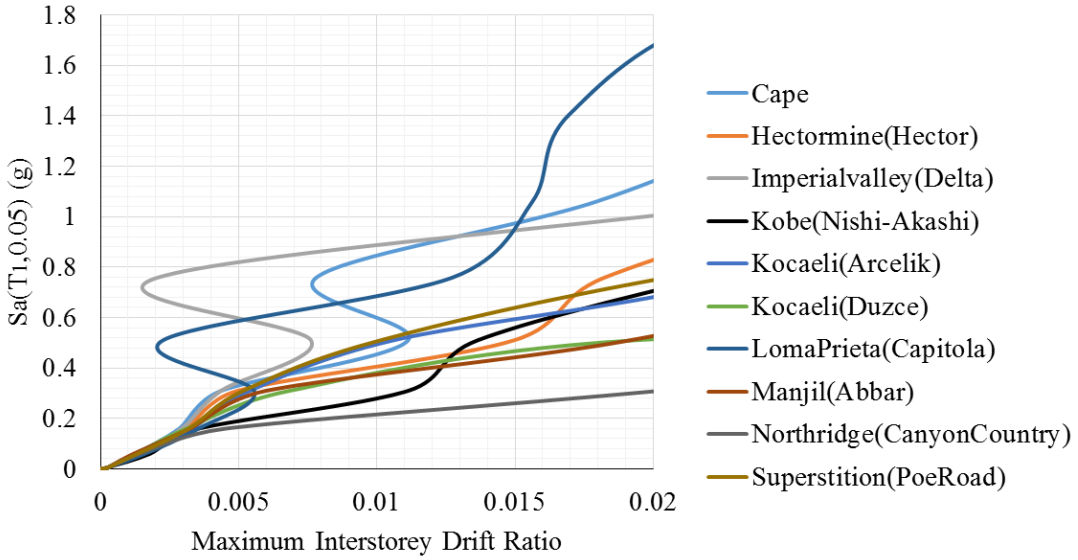

Figure 16

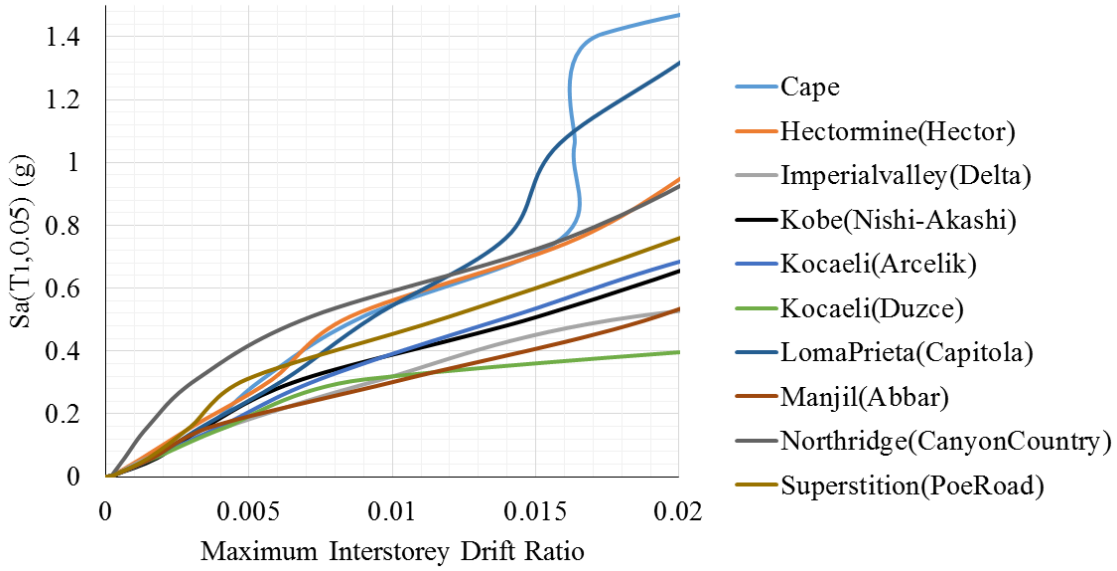

Figure 17

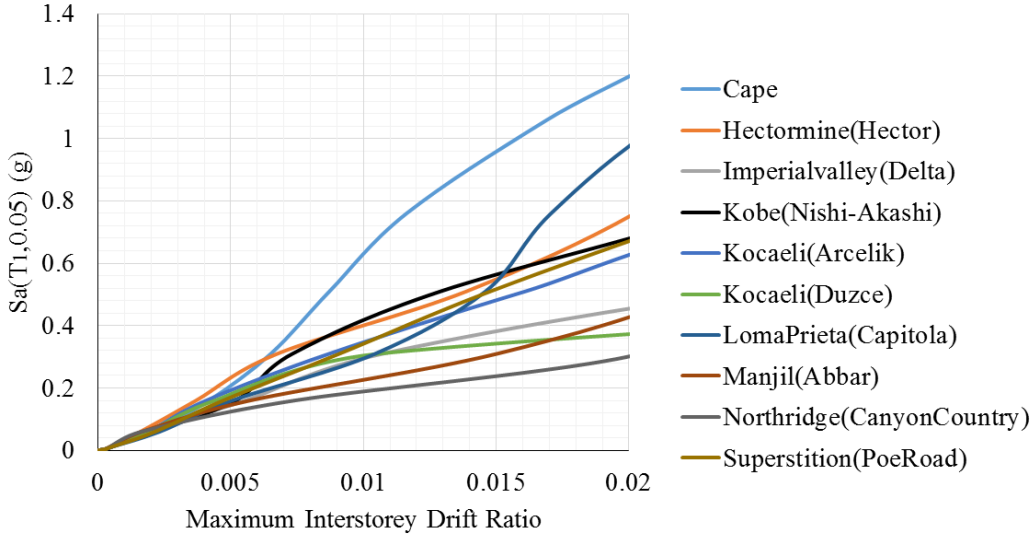

Figure 18

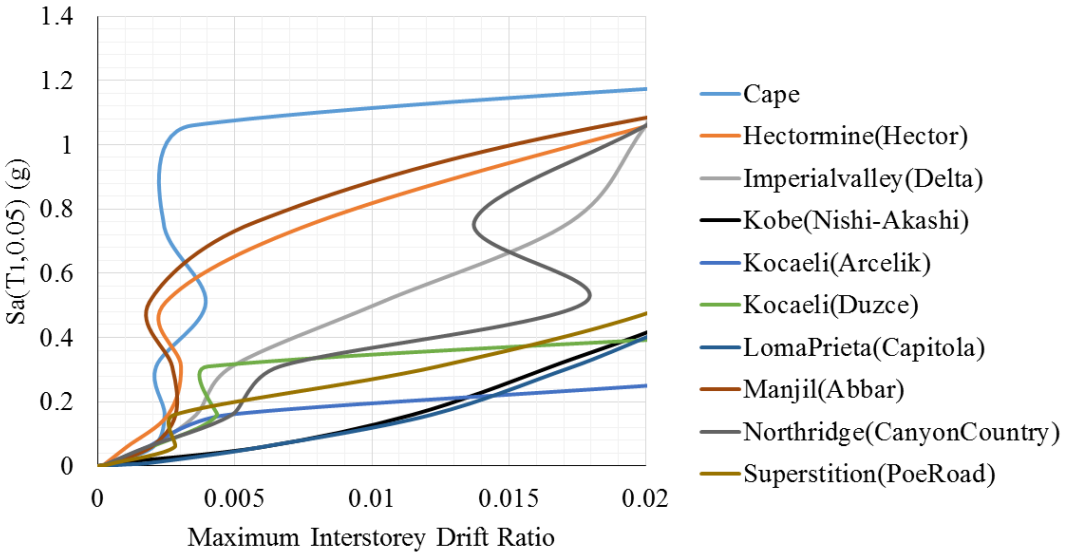

Figure 19

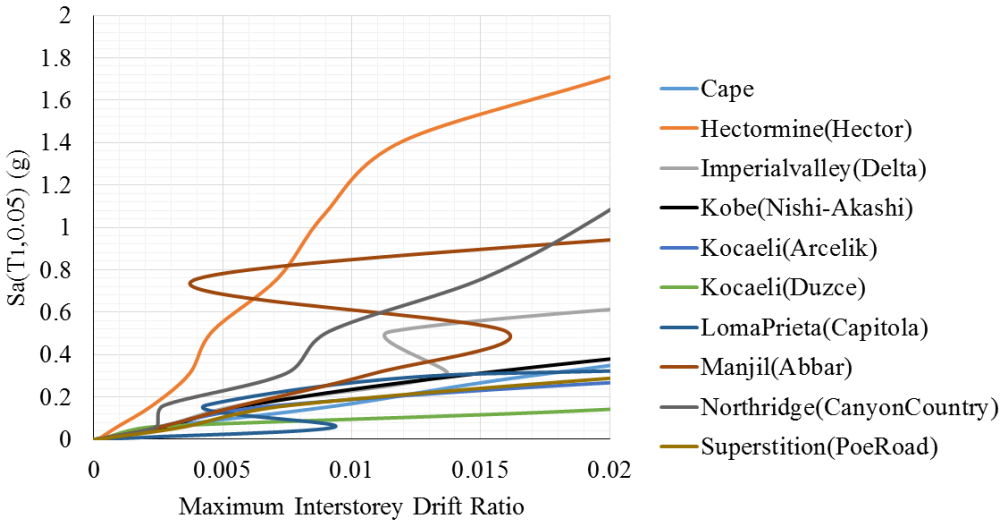

Figure 20

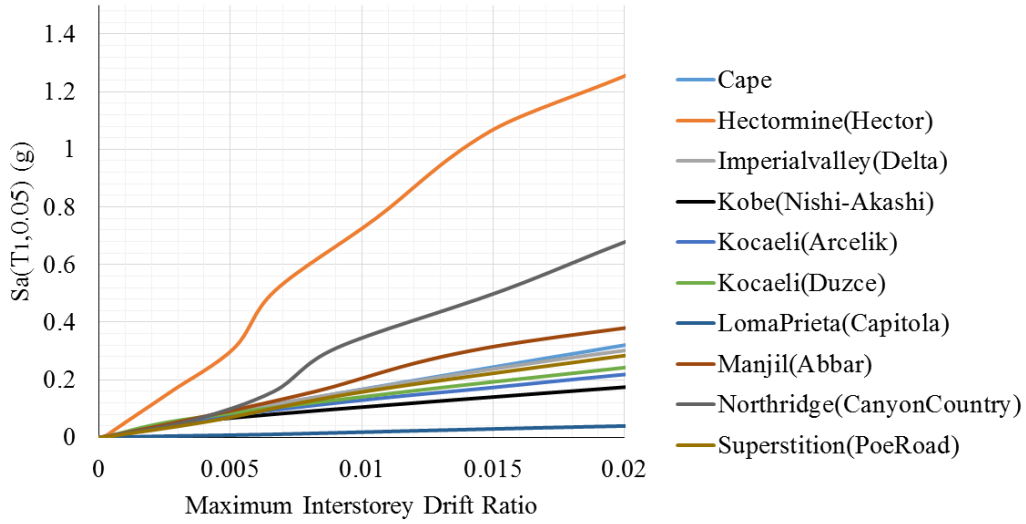

Figure 21

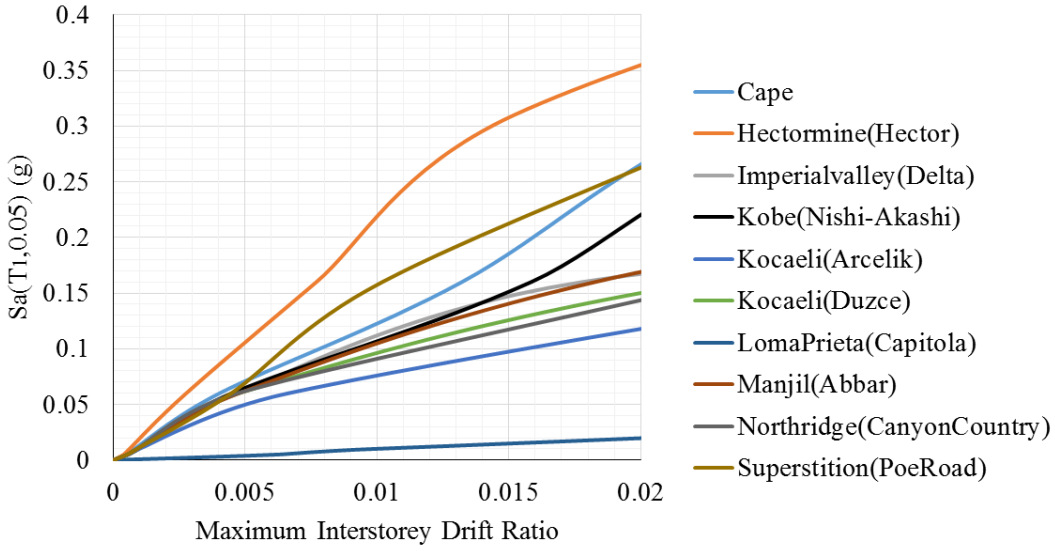

Figure 22

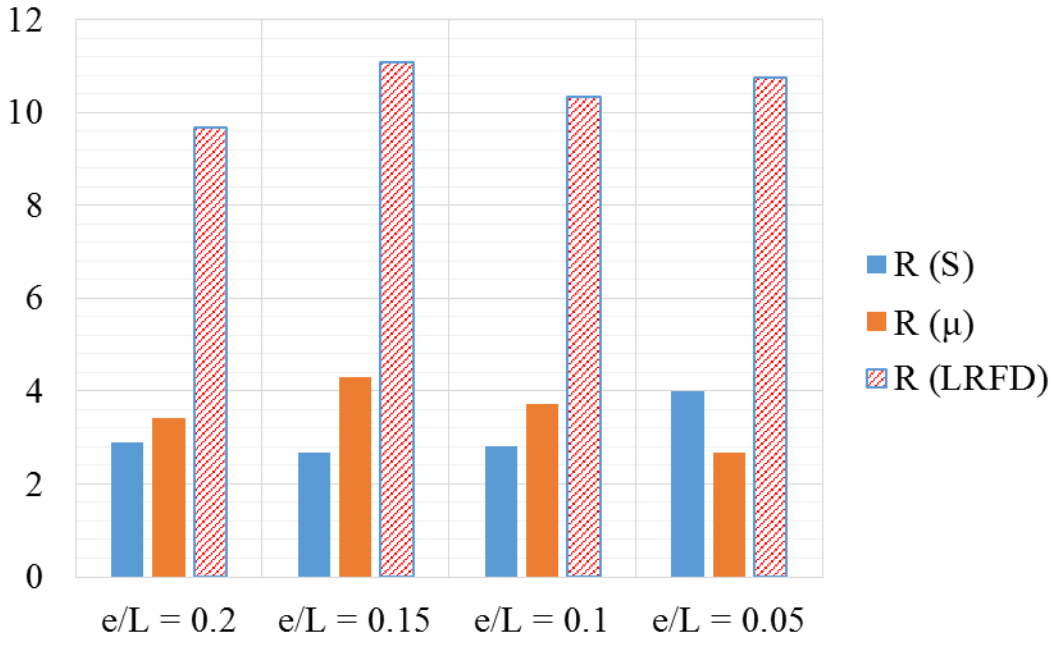

Figure 23

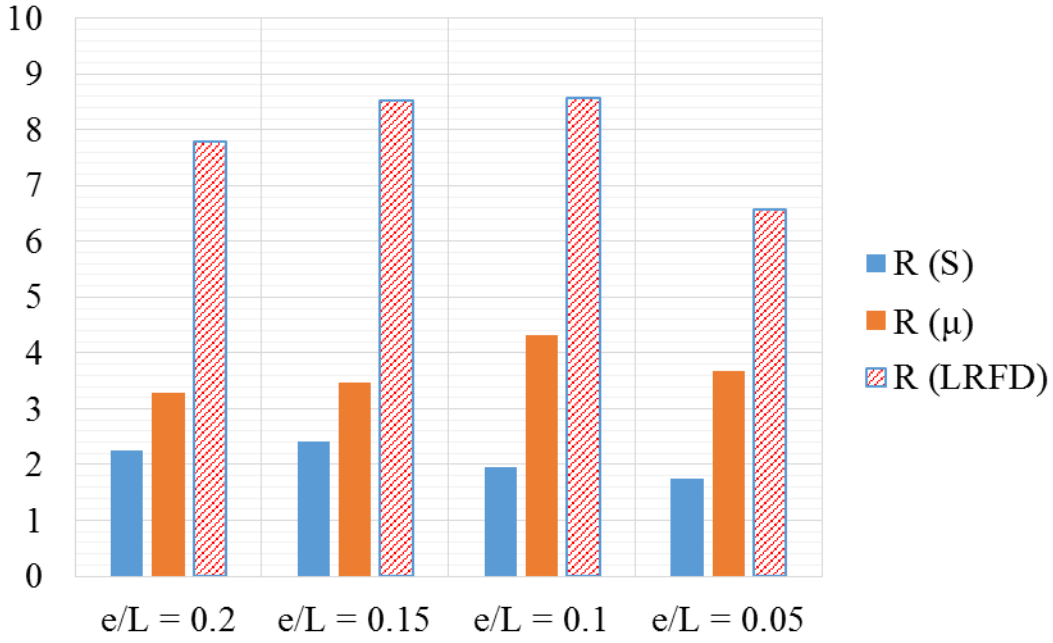

Figure 24

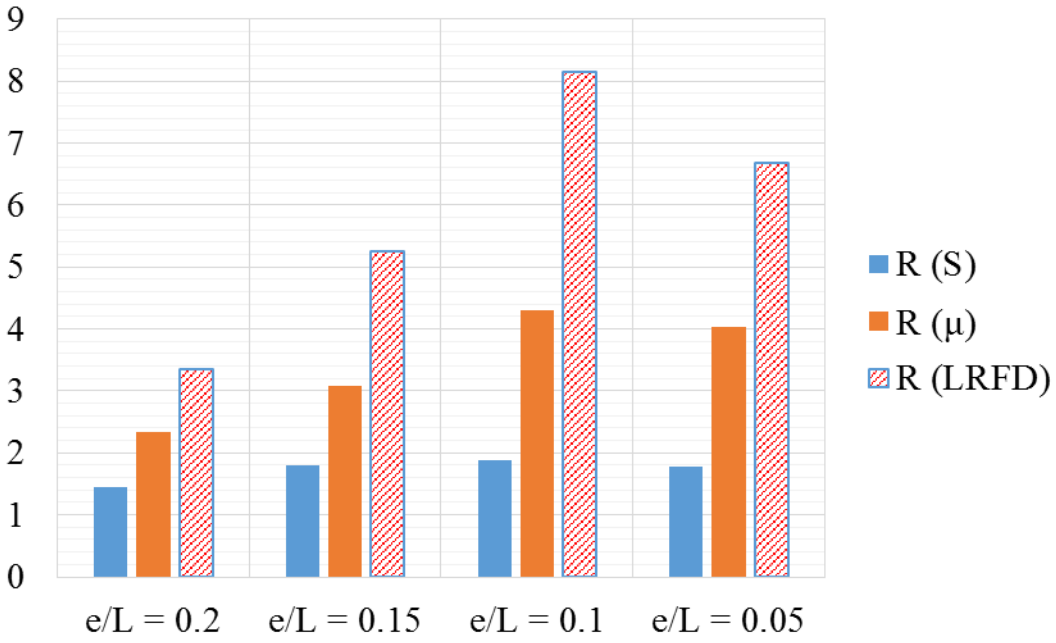

Figure 25

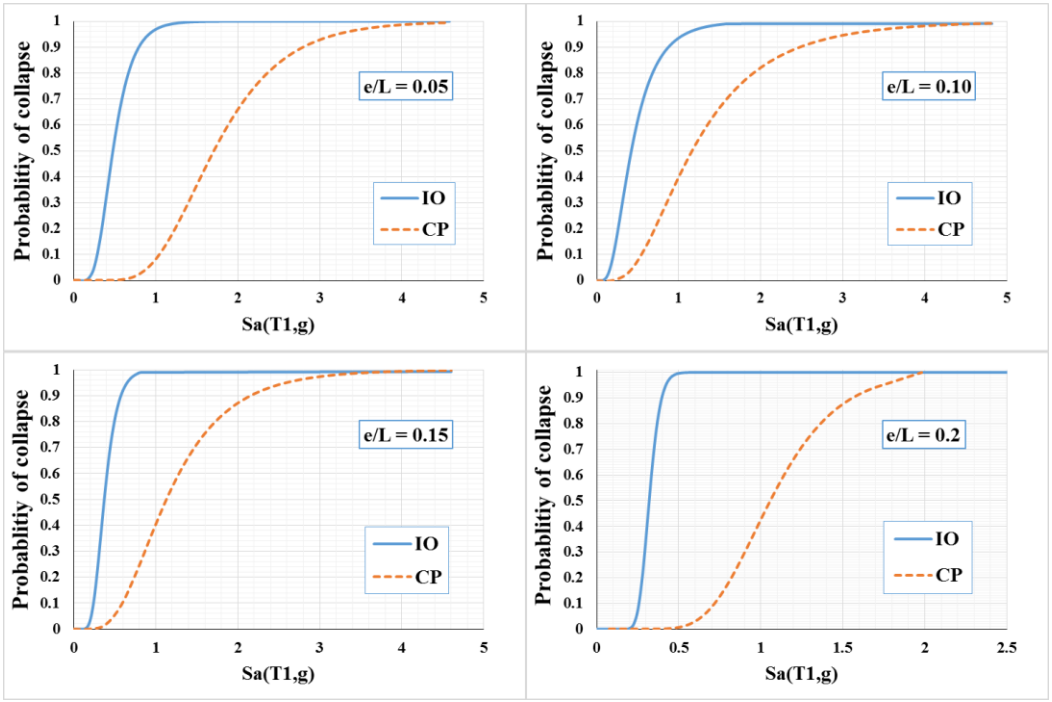

Figure 26

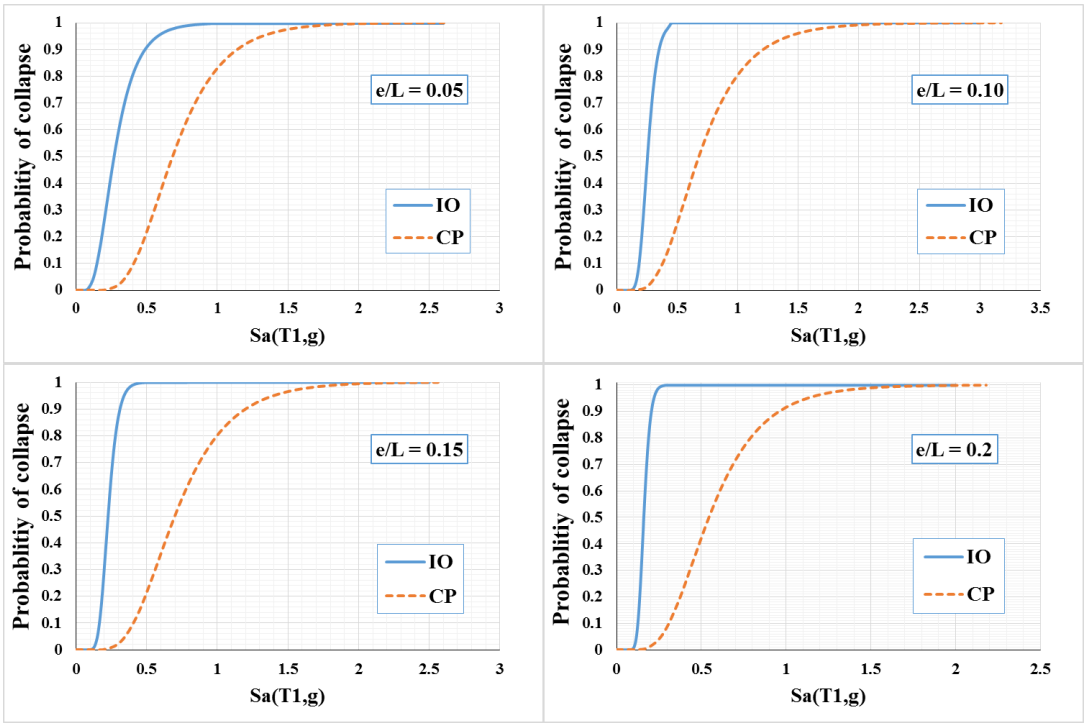

Figure 27

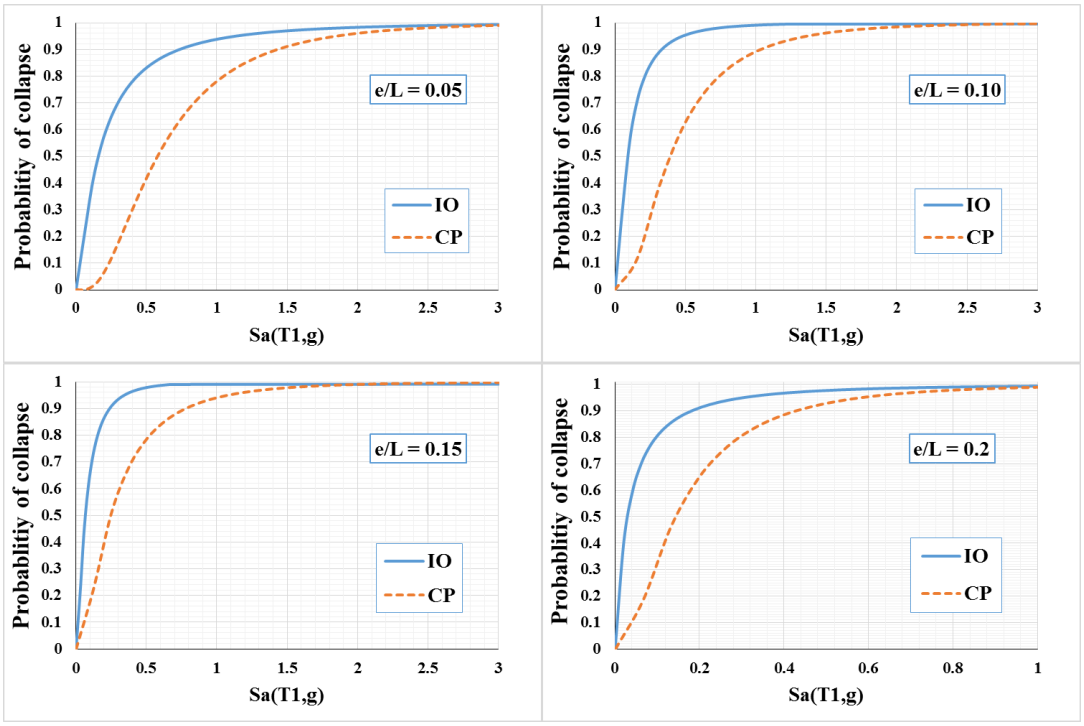

Figure 28

Table 1

Record No.	Record	Record station	Occurrence date	PGA(g)	Mag.	Mechanism	R_{jb}(km)	R_{rup}(km)	Vs30(m/s)	Lowest useable frequency (Hz)
1	Cape Mendocino	Rio Dell Overpass	1992/04/25	0.195	7	Thrust	7.9	7.9	312	0.07
2	Hector mine	Hector	1994/01/17	0.318	7.13	strike slip	10.35	11.66	726	0.0375
3	Imperial valley	Delta	1979/10/15	0.237	6.53	strike slip	22.03	22.03	242.05	0.0875
4	Kobe	Nishi-Akashi	1995/01/16	0.370	6.9	strike slip	7.08	7.08	609	0.125
5	Kocaeli	Arcelik	1999/08/17	0.218	7.51	strike slip	10.56	13.49	523	0.0875
6	Kocaeli	Duzce	1999/08/17	0.229	7.51	strike slip	13.6	15.37	281.86	0.1
7	Loma Prieta	Capitola	1989/10/18	0.541	6.93	Reverse Oblique	8.65	15.23	288.62	0.25
8	Manjil	Abbar	1990/06/20	0.077	7.37	strike slip	12.55	12.55	723.95	0.13
9	Northridge	Canyon Country	1994/01/17	0.318	6.69	Reverse	11.39	12.44	325.6	0.125
10	Superstition	Poe Road	1987/11/24	0.446	6.54	strike slip	11.16	11.16	316.64	0.1625

Table 2

Storey	Side columns	Middle columns	Bracing	Side beams	Beam outside link beam	Link beam
2	W6x12	W5x16	2C5x6.7	W12x19	PG2-1	PL2-1
1	W6x12	W5x16	2C6x8.2	W12x19	PG2-1	PL2-1

Table 3

Storey	Side columns	Middle columns	Bracing	Side beams	Beam outside link beam	Link beam
6	W6x12	W5x16	2C4x5.4	W12x19	PG6-3	PL6-3
5	W6x12	W5x16	2C6x8.2	W12x19	PG6-3	PL6-3
4	W6x12	W8x40	2C5x9	W12x19	PG6-2	PL6-2
3	W4x13	W8x40	2C7x9.8	W12x19	PG6-2	PL6-2
2	W5x16	W18x86	2C7x9.8	W12x19	PG6-1	PL6-1
1	W5x16	W18x86	2C6x10.5	W12x19	PG6-1	PL6-1

Table 4

Storey	Side columns	Middle columns	Bracing	Side beams	Beam outside ink beam	Link beam
10	W6x12	W5x16	2C3x5	W12x19	PG10-5	PL10-5
9	W6x12	W5x16	2C4x7.25	W12x19	PG10-5	PL10-5
8	W6x12	W8x67	2C7x9.8	W12x19	PG10-4	PL10-4
7	W4x13	W8x67	2C5x9	W12x19	PG10-4	PL10-4
6	W5x16	W18x130	2C5x9	W12x19	PG10-3	PL10-3
5	W5x16	W18x86	2C8x11.5	W12x19	PG10-3	PL10-3
4	W5x16	W14x193	2C6x10.5	W12x19	PG10-2	PL10-2
3	W5x19	W14x132	2C9x13.4	W12x19	PG10-2	PL10-2
2	W8x21	W14x193	2C9x13.4	W12x19	PG10-1	PL10-1
1	W6x25	W14x193	2C9x13.4	W12x19	PG10-1	PL10-1

Table 5

Plate girder	Web height (cm)	Web thickness (cm)	Flange width (cm)	Flange thickness (cm)	Plate girder	Web height (cm)	Web thickness (cm)	Flange width (cm)	Flange thickness (cm)
PG2-1	45	0.9	20	0.8	PL2-1	45	0.9	20	0.5
PG6-1	45	1.1	20	0.8	PL6-1	45	1.1	20	0.5
PG6-2	40	0.9	20	0.8	PL6-2	40	0.9	20	0.5
PG6-3	25	0.8	20	0.9	PL6-3	25	0.8	20	0.5
PG10-1	45	1.4	20	1	PL10-1	45	1.4	20	0.6
PG10-2	45	1.3	20	1	PL10-2	45	1.3	20	0.5
PG10-3	45	1.1	20	0.8	PL10-3	45	1.1	20	0.5
PG10-4	40	0.9	20	0.8	PL10-4	40	0.9	20	0.5
PG10-5	25	0.7	20	0.8	PL10-5	25	0.7	20	0.5

Table 6

Record	Recording station	$V_{b(Dyn,u)}$ (ton)	$V_{b(st,y)}$ (ton)	$V_{b(Dyn,el)}$ (ton)	R_μ	R_S	R_{LRFD}	R_{ASD}
Cape Mendocino	Rio Dell Overpass	119.54	27.73	250.06	2.09	4.31	9.02	12.62
Hector mine	Hector	115.99	27.73	277.86	2.40	4.18	10.02	14.03
Imperial valley	Delta	118.63	27.73	265.72	2.24	4.28	9.58	13.42
Kobe	Nishi-Akashi	120.15	27.73	467.92	3.89	4.33	16.87	23.62
Kocaeli	Arcelik	91.87	27.73	195.73	2.13	3.31	7.06	9.88
Kocaeli	Duzce	100.95	27.73	277.05	2.74	3.64	9.99	13.99
Loma Prieta	Capitola	118.84	27.73	473.32	3.98	4.29	17.07	23.90
Manjil	Abbar	115.35	27.73	194.79	1.69	4.16	7.02	9.83
Northridge	Canyon Country	108.60	27.73	310.00	2.85	3.92	11.18	15.65
Superstition	Poe Road	98.33	27.73	270.38	2.75	3.55	9.75	13.65
Average					2.68	4.00	10.76	15.06
σ					1.03	1.16	3.51	4.92
C.V.					0.39	0.29	0.33	0.33

Table 7

Record	Recording station	$V_{b(Dyn,u)}$ (ton)	$V_{b(st,y)}$ (ton)	$V_{b(Dyn,el)}$ (ton)	R_μ	R_S	R_{LRFD}	R_{ASD}
Cape Mendocino	Rio Dell Overpass	49.20	22.84	152.87	3.11	2.15	6.69	9.37
Hector mine	Hector	62.52	22.84	181.24	2.90	2.74	7.94	11.11
Imperial valley	Delta	44.45	22.84	180.82	4.07	1.95	7.92	11.08
Kobe	Nishi-Akashi	78.53	22.84	433.52	5.52	3.44	18.98	26.57
Kocaeli	Arcelik	72.22	22.84	190.94	2.64	3.16	8.36	11.70
Kocaeli	Duzce	61.03	22.84	211.62	3.47	2.67	9.27	12.97
Loma Prieta	Capitola	113.77	22.84	343.36	3.02	4.98	15.03	21.05
Manjil	Abbar	52.03	22.84	143.92	2.77	2.28	6.30	8.82
Northridge	Canyon Country	55.94	22.84	219.73	3.93	2.45	9.62	13.47
Superstition	Poe Road	53.81	22.84	305.84	5.68	2.36	13.39	18.75
Average					3.71	2.82	10.35	14.49
σ					1.08	0.84	3.97	5.55
C.V.					0.29	0.30	0.38	0.38

Table 8

Record	Recording station	$V_{b(Dyn,u)}$ (ton)	$V_{b(st,y)}$ (ton)	$V_{b(Dyn,el)}$ (ton)	R_μ	R_S	R_{LRFD}	R_{ASD}
Cape Mendocino	Rio Dell Overpass	55.02	22.34	143.07	2.60	2.46	6.40	8.97
Hector mine	Hector	57.74	22.34	326.27	5.65	2.58	14.60	20.45
Imperial valley	Delta	40.07	22.34	155.09	3.87	1.79	6.94	9.72
Kobe	Nishi-Akashi	62.85	22.34	429.24	6.83	2.81	19.21	26.90
Kocaeli	Arcelik	72.93	22.34	243.29	3.34	3.26	10.89	15.25
Kocaeli	Duzce	53.83	22.34	110.58	2.05	2.41	4.95	6.93
Loma Prieta	Capitola	111.66	22.34	279.19	2.50	5.00	12.50	17.50
Manjil	Abbar	46.73	22.34	157.27	3.37	2.09	7.04	9.86
Northridge	Canyon Country	50.67	22.34	213.21	4.21	2.27	9.54	13.36
Superstition	Poe Road	48.89	22.34	417.12	8.53	2.19	18.67	26.14
Average					4.29	2.69	11.08	15.51
σ					2.17	0.88	5.03	7.04
C.V.					0.50	0.33	0.45	0.45

Table 9

Record	Recording station	$V_{b(Dyn,u)}$ (ton)	$V_{b(st,y)}$ (ton)	$V_{b(Dyn,el)}$ (ton)	R_μ	R_S	R_{LRFD}	R_{ASD}
Cape Mendocino	Rio Dell Overpass	70.31	21.67	160.72	2.29	3.24	7.42	10.38
Hector mine	Hector	64.68	21.67	223.94	3.46	2.98	10.33	14.47
Imperial valley	Delta	49.64	21.67	233.83	4.71	2.29	10.79	15.11
Kobe	Nishi-Akashi	69.34	21.67	378.00	5.45	3.20	17.44	24.42
Kocaeli	Arcelik	68.35	21.67	244.06	3.57	3.15	11.26	15.77
Kocaeli	Duzce	50.85	21.67	93.73	1.84	2.35	4.33	6.06
Loma Prieta	Capitola	101.50	21.67	225.49	2.22	4.68	10.41	14.57
Manjil	Abbar	50.21	21.67	125.08	2.49	2.32	5.77	8.08
Northridge	Canyon Country	51.51	21.67	170.92	3.32	2.38	7.89	11.04
Superstition	Poe Road	49.41	21.67	241.24	4.88	2.28	11.13	15.59
Average					3.42	2.89	9.68	13.55
σ					1.18	0.72	3.45	4.84
C.V.					0.35	0.25	0.36	0.36

Table 10

Record	Recording station	$V_{b(Dyn,u)}$ (ton)	$V_{b(st,y)}$ (ton)	$V_{b(Dyn,el)}$ (ton)	R_μ	R_S	R_{LRFD}	R_{ASD}
Cape Mendocino	Rio Dell Overpass	86.95	46.50	521.12	5.99	1.87	11.21	15.69
Hector mine	Hector	85.36	46.50	108.06	1.27	1.84	2.32	3.25
Imperial valley	Delta	77.40	46.50	326.99	4.22	1.66	7.03	9.84
Kobe	Nishi-Akashi	112.04	46.50	355.89	3.18	2.41	7.65	10.71
Kocaeli	Arcelik	94.40	46.50	569.02	6.03	2.03	12.24	17.13
Kocaeli	Duzce	68.08	46.50	270.22	3.97	1.46	5.81	8.14
Loma Prieta	Capitola	85.04	46.50	435.57	5.12	1.83	9.37	13.11
Manjil	Abbar	46.80	46.50	136.87	2.92	1.01	2.94	4.12
Northridge	Canyon Country	66.69	46.50	104.50	1.57	1.43	2.25	3.15
Superstition	Poe Road	89.40	46.50	229.41	2.57	1.92	4.93	6.91
Average					3.68	1.75	6.58	9.21
σ					1.65	0.62	3.61	5.06
C.V.					0.45	0.36	0.55	0.55

Table 11

Record	Recording station	$V_{b(Dyn,u)}$ (ton)	$V_{b(st,y)}$ (ton)	$V_{b(Dyn,el)}$ (ton)	R_μ	R_S	R_{LRFD}	R_{ASD}
Cape Mendocino	Rio Dell Overpass	75.78	45.84	391.52	5.17	1.65	8.54	11.96
Hector mine	Hector	88.08	45.84	438.31	4.98	1.92	9.56	13.39
Imperial valley	Delta	80.84	45.84	527.96	6.53	1.76	11.52	16.12
Kobe	Nishi-Akashi	100.25	45.84	482.97	4.82	2.19	10.54	14.75
Kocaeli	Arcelik	86.16	45.84	416.39	4.83	1.88	9.08	12.72
Kocaeli	Duzce	77.03	45.84	270.81	3.52	1.68	5.91	8.27
Loma Prieta	Capitola	129.51	45.84	708.65	5.47	2.83	15.46	21.64
Manjil	Abbar	82.55	45.84	222.90	2.70	1.80	4.86	6.81
Northridge	Canyon Country	84.94	45.84	156.38	1.84	1.85	3.41	4.78
Superstition	Poe Road	92.05	45.84	317.69	3.45	2.01	6.93	9.70
Average					4.33	1.96	8.58	12.01
σ					1.69	0.44	3.43	4.81
C.V.					0.39	0.22	0.40	0.40

Table 12

Record	Recording station	$V_{b(Dyn,u)}$ (ton)	$V_{b(st,y)}$ (ton)	$V_{b(Dyn,el)}$ (ton)	R_μ	R_S	R_{LRFD}	R_{ASD}
Cape Mendocino	Rio Dell Overpass	114.02	44.71	592.74	5.20	2.55	13.26	18.56
Hector mine	Hector	117.84	44.71	453.17	3.85	2.64	10.14	14.19
Imperial valley	Delta	96.27	44.71	433.05	4.50	2.15	9.69	13.56
Kobe	Nishi-Akashi	119.76	44.71	444.82	3.71	2.68	9.95	13.93
Kocaeli	Arcelik	86.72	44.71	301.14	3.47	1.94	6.74	9.43
Kocaeli	Duzce	85.82	44.71	224.77	2.62	1.92	5.03	7.04
Loma Prieta	Capitola	129.77	44.71	672.29	5.18	2.90	15.04	21.05
Manjil	Abbar	107.58	44.71	230.91	2.15	2.41	5.16	7.23
Northridge	Canyon Country	114.45	44.71	158.81	1.39	2.56	3.55	4.97
Superstition	Poe Road	108.78	44.71	296.93	2.73	2.43	6.64	9.30
Average					3.48	2.42	8.52	11.93
σ					1.22	0.35	3.62	5.07
C.V.					0.35	0.14	0.43	0.43

Table 13

Record	Recording station	$V_{b(Dyn,u)}$ (ton)	$V_{b(st,y)}$ (ton)	$V_{b(Dyn,el)}$ (ton)	R_μ	R_S	R_{LRFD}	R_{ASD}
Cape Mendocino	Rio Dell Overpass	108.23	41.84	486.79	4.50	2.59	11.63	16.29
Hector mine	Hector	96.48	41.84	325.58	3.37	2.31	7.78	10.89
Imperial valley	Delta	86.51	41.84	235.77	2.73	2.07	5.64	7.89
Kobe	Nishi-Akashi	98.74	41.84	349.23	3.54	2.36	8.35	11.69
Kocaeli	Arcelik	81.77	41.84	296.48	3.63	1.95	7.09	9.92
Kocaeli	Duzce	74.73	41.84	164.30	2.20	1.79	3.93	5.50
Loma Prieta	Capitola	127.18	41.84	752.77	5.92	3.04	17.99	25.19
Manjil	Abbar	92.50	41.84	216.75	2.34	2.21	5.18	7.25
Northridge	Canyon Country	80.84	41.84	148.46	1.84	1.93	3.55	4.97
Superstition	Poe Road	95.58	41.84	277.94	2.91	2.28	6.64	9.30
Average					3.30	2.25	7.78	10.89
$\boldsymbol{\sigma}$					1.15	0.35	4.07	5.69
C.V.					0.35	0.15	0.52	0.52

Table 14

Record	Recording station	$V_{b(Dyn,u)}$ (ton)	$V_{b(st,y)}$ (ton)	$V_{b(Dyn,el)}$ (ton)	R_μ	R_S	R_{LRFD}	R_{ASD}
Cape Mendocino	Rio Dell Overpass	81.69	52.88	81.69	1.00	1.54	1.54	2.16
Hector mine	Hector	112.09	52.88	653.82	5.83	2.12	12.36	17.31
Imperial valley	Delta	120.42	52.88	526.43	4.37	2.28	9.96	13.94
Kobe	Nishi-Akashi	120.91	52.88	120.91	1.00	2.29	2.29	3.20
Kocaeli	Arcelik	82.95	52.88	211.76	2.55	1.57	4.00	5.61
Kocaeli	Duzce	106.65	52.88	238.92	2.24	2.02	4.52	6.33
Loma Prieta	Capitola	60.75	52.88	755.08	12.43	1.15	14.28	19.99
Manjil	Abbar	64.60	52.88	150.37	2.33	1.22	2.84	3.98
Northridge	Canyon Country	80.03	52.88	385.03	4.81	1.51	7.28	10.19
Superstition	Poe Road	111.58	52.88	411.13	3.68	2.11	7.77	10.88
Average					4.02	1.78	6.69	9.36
σ					3.60	0.53	5.35	7.49
C.V.					0.89	0.30	0.80	0.80

Table 15

Record	Recording station	$V_{b(Dyn,u)}$ (ton)	$V_{b(st,y)}$ (ton)	$V_{b(Dyn,el)}$ (ton)	R_μ	R_S	R_{LRFD}	R_{ASD}
Cape Mendocino	Rio Dell Overpass	108.76	50.46	317.49	2.92	2.16	6.29	8.81
Hector mine	Hector	103.17	50.46	396.18	3.84	2.04	7.85	10.99
Imperial valley	Delta	99.97	50.46	428.52	4.29	1.98	8.49	11.89
Kobe	Nishi-Akashi	106.52	50.46	378.54	3.55	2.11	7.50	10.50
Kocaeli	Arcelik	104.01	50.46	245.89	2.36	2.06	4.87	6.82
Kocaeli	Duzce	54.51	50.46	127.90	2.35	1.08	2.53	3.55
Loma Prieta	Capitola	102.25	50.46	987.16	9.65	2.03	19.56	27.39
Manjil	Abbar	83.89	50.46	345.78	4.12	1.66	6.85	9.59
Northridge	Canyon Country	83.71	50.46	615.02	7.35	1.66	12.19	17.06
Superstition	Poe Road	107.63	50.46	268.02	2.49	2.13	5.31	7.44
Average					4.29	1.89	8.15	11.40
σ					3.00	0.55	6.58	9.22
C.V.					0.70	0.29	0.81	0.81

Table 16

Record	Recording station	$V_{b(Dyn,u)}$ (ton)	$V_{b(st,y)}$ (ton)	$V_{b(Dyn,el)}$ (ton)	R_μ	R_S	R_{LRFD}	R_{ASD}
Cape Mendocino	Rio Dell Overpass	77.82	49.03	186.75	2.40	1.59	3.81	5.33
Hector mine	Hector	89.36	49.03	326.90	3.66	1.82	6.67	9.33
Imperial valley	Delta	84.11	49.03	240.80	2.86	1.72	4.91	6.88
Kobe	Nishi-Akashi	103.97	49.03	205.97	1.98	2.12	4.20	5.88
Kocaeli	Arcelik	97.14	49.03	139.01	1.43	1.98	2.84	3.97
Kocaeli	Duzce	86.62	49.03	149.26	1.72	1.77	3.04	4.26
Loma Prieta	Capitola	98.85	49.03	333.01	3.37	2.02	6.79	9.51
Manjil	Abbar	79.01	49.03	215.04	2.72	1.61	4.39	6.14
Northridge	Canyon Country	66.36	49.03	541.49	8.16	1.35	11.04	15.46
Superstition	Poe Road	98.20	49.03	239.96	2.44	2.00	4.89	6.85
Average					3.08	1.80	5.26	7.36
σ					1.96	0.42	2.99	4.19
C.V.					0.64	0.24	0.57	0.57

Table 17

Record	Recording station	$V_{b(Dynn,u)}$ (ton)	$V_{b(st,y)}$ (ton)	$V_{b(Dyn,el)}$ (ton)	R_μ	R_S	R_{LRFD}	R_{ASD}
Cape Mendocino	Rio Dell Overpass	67.41	48.21	156.90	2.33	1.40	3.25	4.56
Hector mine	Hector	70.66	48.21	161.49	2.29	1.47	3.35	4.69
Imperial valley	Delta	62.93	48.21	138.01	2.19	1.31	2.86	4.01
Kobe	Nishi-Akashi	90.80	48.21	209.89	2.31	1.88	4.35	6.10
Kocaeli	Arcelik	75.86	48.21	131.11	1.73	1.57	2.72	3.81
Kocaeli	Duzce	64.82	48.21	130.94	2.02	1.34	2.72	3.80
Loma Prieta	Capitola	71.38	48.21	182.48	2.56	1.48	3.79	5.30
Manjil	Abbar	61.34	48.21	134.06	2.19	1.27	2.78	3.89
Northridge	Canyon Country	50.56	48.21	155.83	3.08	1.05	3.23	4.53
Superstition	Poe Road	78.77	48.21	211.43	2.68	1.63	4.39	6.14
Average					2.34	1.44	3.34	4.68
σ					0.35	0.22	0.60	0.85
C.V.					0.15	0.15	0.18	0.18

Table 18

Storey numbers	e/L	R_μ	R_s	R_{LRFD}	R_{ASD}
2	0.2	3.42	2.89	9.68	13.55
	0.15	4.29	2.69	11.08	15.51
	0.1	3.71	2.82	10.35	14.49
	0.05	2.68	4.00	10.76	15.06
6	0.2	3.30	2.25	7.78	10.89
	0.15	3.48	2.42	8.52	11.93
	0.1	4.33	1.96	8.58	12.01
	0.05	3.68	1.75	6.58	9.21
10	0.2	2.34	1.44	3.34	4.68
	0.15	3.08	1.80	5.26	7.36
	0.1	4.29	1.89	8.15	11.40
	0.05	4.02	1.78	6.69	9.36
Mean		3.55	2.31	8.06	11.29

$S_a\ (T_1)$ = Spectrum Acceleration for First Period

R_μ = Ductility factor

R_s = Overstrength factor

R_{LRFD} = Response modification factor

e = Length of eccentrically beam

L = Length of spam

$V_{b(Dyn,u)}$ = Maximum nonlinear base shear force in dynamic analysis

$V_{b(Dyn,el)}$ = Maximum linear base shear force in dynamic analysis

Y = Allowable stress factor

V_y = Base shear force of yielding

V_s = Base shear force of first point of Yielding

V_w = Code limitation of base shear

D_{Si} = Occurrence probability of damage status

Φ = Standard accumulative lognormal distribution function

x = Spectral acceleration with lognormal distribution

λ and β = average and standard deviation of ln x